Journal Pre-proof

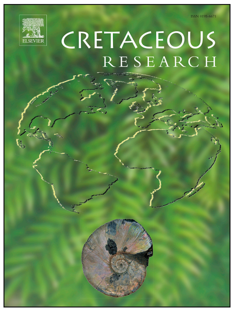

Paleosols of the Maastrichtian dinosaur-bearing Chorrillo Formation (southern Patagonia, Argentina): paleoenvironmental and paleoclimate implications

M. Sol Raigemborn, Sabrina Lizzoli, Damián Moyano-Paz, Augusto N. Varela, Daniel G. Poiré, Valeria, Ezequiel Vera, Makoto Manabe, Fernando Novas

PII: S0195-6671(23)00115-5

DOI: https://doi.org/10.1016/j.cretres.2023.105587

Reference: YCRES 105587

To appear in: *Cretaceous Research*

Received Date: 29 December 2022

Revised Date: 14 April 2023

Accepted Date: 21 May 2023

Paleosols of the Maastrichtian dinosaur-bearing Chorrillo Formation (southern Patagonia, Argentina): paleoenvironmental and paleoclimate implications

M. Sol Raigemborn[1*], Sabrina Lizzoli[2], Damián Moyano-Paz[3], Augusto N. Varela[4], Daniel G. Poiré[3], Valeria [5], Ezequiel Vera[5,6], Makoto Manabe[7] and Fernando Novas[8]

[1]CONICET – UNLP. Centro de Investigaciones Geológicas, Diagonal 113 n.o 275 (1900) La Plata, Argentina, and Cátedra de Micromorfología de Suelos, Facultad de Ciencias Naturales y Museo, UNLP, Calle 122 y 60 s/n, (1900) La Plata, Argentina. msol@cig.museo.unlp.edu.ar

[2]CONICET – UNLP. Centro de Investigaciones Geológicas, Diagonal 113 n.o 275 (1900) La Plata, Argentina, and Cátedra de Pedología General, Facultad de Ciencias Naturales y Museo, UNLP, Calle 122 y 60 s/n (1900) La Plata, Argentina. slizzoli@cig.museo.unlp.edu.ar

[3]CONICET – UNLP. Centro de Investigaciones Geológicas, Diagonal 113 n.o 275 (1900) La Plata, Argentina, and Cátedra de Sedimentología, Facultad de Ciencias Naturales y Museo, UNLP, Calle 122 y 60 s/n (1900) La Plata, Argentina. dmoyanopaz@cig.museo.unlp.edu.ar,

[4]Y-TEC (YPF Tecnología) Av. Del Petróleo s/n (1923), Berisso, Argentina, and Cátedra de Micromorfología de Suelos, Facultad de Ciencias Naturales y Museo, Universidad Nacional de La Plata, Calle 122 y 60 s/n, (1900) La Plata, Argentina. augusto.n.varela@ypftecnologia.com

[5]División Paleobotánica, Museo Argentino de Ciencias Naturales "Bernardino Rivadavia" (CONICET), Av. Angel Gallardo 470, Ciudad Autónoma de Buenos Aires, C1405DJR, Argentina. loinazev@gmail.com

[6]Área de Paleontología, Departamento de Ciencias Geológicas, Universidad de Buenos Aires, Pabellón 2, Ciudad Universitaria, Buenos Aires, C1428EGA, Argentina ezequiel.vera@gmail.com

[7]Center for the Collections, Natural Museum of Nature & Science, Tsukuba 305-0005, Japan. makotosaurus@gmail.com

[8]Laboratorio de Anatomía Comparada y Evolución de los Vertebrados del Museo Argentino de Ciencias Naturales "Bernardino Rivadavia" (CONICET), Av. Ángel Gallardo 470, C1405DJR, Ciudad Autónoma de Buenos Aires, Argentina. fernovas@yahoo.com.ar

* Corresponding author. Tel and Fax: (+54) 221 6441230

E-mail address: msol@cig.museo.unlp.edu.ar (M.S. Raigemborn)

ABSTRACT

The Maastrichtian dinosaur-bearing Chorrillo Formation in southern Patagonia (~50° S, Austral-Magallanes Basin, Argentina) is a pedogenically modified fluvial succession, which records sediment deposition at mid–high paleolatitudes in the Southern Hemisphere. In order to reconstruct the paleoenvironment and paleoclimates for the Chorrillo Formation, we performed a paleopedological study (abiotic components) of the unit within a well-defined sedimentological-paleontological context, and considering new paleobotanical data of the unit. Using detailed macro and micromorphological features and clay mineralogy of the paleosols, we show that the Chorrillo Formation paleosols are overall smectite-rich soils with vertic and redoximorphic features (i.e., moderately developed hydromorphic Vertisol-, calcic Vertisol-, poorly developed hydromorphic Vertisol-, Histosol-, and argillic Vertisol-like paleosols). The small-scale or high-frequency stacking of such paleosols indicates that they developed under different hydrologic conditions, and subtle differences in grain-size (parent material) and topographic relief on a distal floodplain. Conversely, the large-scale or small-frequency vertical stacking of different paleosols is linked to avulsion processes. Paleobotanical remains through the Chorrillo succession demonstrates different ecological requirements for the inhabited part of the fluvial floodplain. Abiotic and biotic climate proxies suggest that these paleosols formed under a broadly temperate–warm and seasonally humid climate. Overall, these combined data record environmental and climatic conditions during the uppermost Cretaceous, and preserve a record of Maastrichtian terrestrial conditions in the Southern Hemisphere.

Keywords: Micromorphology, Clay-mineralogy, Hydromorphism, Vertisols, Palynology, Cretaceous

1. Introduction

Integration of paleopedological and sedimentological data makes up a powerful interpretative tool to understand environmental conditions and landscape evolution (e.g., Kraus and Aslan, 1993, 1999; Kraus, 1997; Wright et al., 2000; Licht et al., 2013; Raigemborn et al., 2018a, c). The relationship between paleosols and sedimentary processes at different scale in a fluvial succession responds to autocyclic (i.e., avulsion, lateral channel migrations, crevassing, development of soil catenas) and allocyclic (i.e., eustatic sea-level, tectonism, climate) factors (e.g., Wright and Marriott, 1993; Kraus and Aslan, 1999; Kraus, 1999; Raigemborn et al., 2018a; Varela et al., 2021). Although the catena model is considered the most standard association in floodplain deposits, this paleosols-landscape association do not satisfactory explain lateral relations in all floodplain-paleosol succession, and do not can be apply in exposures that prevent a detailed lateral study (e.g., Kraus, 1999; Wright et al., 2000; Licht et al., 2013). Alternatively, variations of hydromorphic features in fine-grained alluvial deposits can be used as a model of distribution of hydromophy in such deposits to the reconstruction of overbank floodplain paleoenvironments (e.g., Licht et al., 2013).

The Chorrillo Formation (Maastrichtian, Austral-Magallanes Basin at the Lago Argentino area, southern Argentina; Fig. 1) is an important dinosaur-bearing unit of Patagonia (Feruglio, 1945). The sedimentological aspects of this important dinosaur-bearing unit of Patagonia were newly addressed by Moyano-Paz et al. (2022a), in which a detailed characterization of the channelized fluvial deposits of the unit was conducted. However, up to now no detailed studies were carried out the non-channelized and pedogenically modified fine-grained deposits of the Chorrillo Formation, which represent more than the 60% of the unit, and consequently, environmental and climatic conditions of this unit still remained unstudied. .

We applied the combined use of macro- and micromorphology, and clay mineralogy of the Chorillo Formation paleosols, considering the sedimentological and paleontological context (i.e., paleovertebrate and paleobotanical data) and new palynological remains recorded through the unit in order to (1) characterize the paleosols and the pedogenic processes of the unit, (2) reconstruct the Maastrichtian environmental conditions in the non-channelized fine-grained deposits of the Chorrillo Formation, and (3) infer climatic conditions during paleosol formation in southern Patagonia, determining possible variations of environmental and climatic conditions throughout and within the unit.

2. Geological setting and sedimentological-paleontological context

The Austral-Magallanes Basin is located at the most austral extension of Patagonia in South America (Fig. 1A). The tectonic history of the basin consists of three main stages: i) an initial extensional stage (rift) related to the break-up of Gondwana from the Middle to Late Jurassic resulting of isolated depocenters filled with the volcaniclastic deposits of the El Quemado Complex; ii) a postrift thermal subsidence stage (Tithonian-Albian) which is characterized by the deposition of the marine deposits of the Springhill and Río Mayer formations; and finally iii) a compressional phase began near the Albian-Cenomanian boundary (~100Ma) resulting in the development of a retroarc foreland system linked to the growth of the Andes (Biddle et al., 1986; Pankhurst et al., 2000; Varela et al., 2012; Cuitiño et al., 2019).

At the Lago Argentino region (49°40’ to 50°37’ S), southwest of the Santa Cruz province, the onset of the foreland basin is characterized by a thick record of deep marine to coastal strata (e.g., Malkowski et al., 2017; Moyano Paz et al., 2020, 2022b, 2022c; Dobbs et al., 2022). During the late Campanian through Maastrichtian, this region of the basin underwent a complete continentalization (Ghiglione et al., 2021) and exhibits thick fluvial successions assigned to the Cerro Fortaleza, La Irene and Chorrillo formations (Sickmann et al., 2018; Tettamanti et al., 2018; Moyano-Paz et al., 2022a).

The Chorrillo Formation (Maastrichtian) was initially named as 'dinosaur-bearing strata' because of its abundance in fossil vertebrate remains (Feruglio, 1945; Bonaparte, 1996). However, it was in the last of years that there has been a boom in studies focused on the palaeontological content of the unit (Novas et al., 2019; Chimento et al., 2020, 2021; Rozadilla et al., 2021; Aranciaga Rolando et al., 2022; Moyano-Paz et al., 2022a; Vera et al., 2022). This formation is the youngest lithostratigraphic unit that accumulated during the continental expansion of the Austral-Magallanes Basin and crops out to the south of the Lago Argentino (Fig. 1B-C) (Moyano-Paz et al., 2022a). It overlies the coarse-grained braided fluvial deposits of the La Irene Formation (Macellari et al., 1989; Tettamanti et al., 2018) and it is covered by the shallow marine deposits of the Calafate Formation (Fig. 1B) (Odino Barreto et al., 2018).

2.1. Sedimentological and paleontological context

The Chorrillo Formation is a ~500 m thick low gradient fluvial succession dominated by non-channelized units, especially by fine-grained deposits of the distal floodplain which alternate with sandy crevasse splay deposits, and dark fine-grained deposits of swamp or pond settings, and with channelized units (i.e., fluvial channels) (Moyano-Paz et al., 2022a). The fine-grained deposits constitute more than 60% of the total unit and are mainly dark reddish to grey colored and show evidence of both soil development and waterlogging (Moyano-Paz et al., 2022a; Vera et al., 2022; Perez Loinaze et al., 2023; this study).

The lowland area where the Chorrillo Formation accumulated was located near the coastline evidenced by the marine influence recorded by the fluvial deposits of the laterally equivalent Dorotea Formation and contemporaneous fossiliferous site, which crops out in the Última Esperanza region, in southern Chile (Fig. 1A) (Manriquez et al., 2019; Davis et al., 2022). This contemporaneous fossiliferous site in Chile is roughly 20 km south of the study area. There, sites are associated to paleosols developed in fluvial floodplain or tidal flat settings, floodplain and meandering river deposits and nearshore marine settings (Manríquez et al., 2021; Davis et al., 2022).

Despite the proximity with the fluvial-marine transition zone, no marine influence has been described for the Chorrillo Formation deposit except for the presence of marine skeletal remains within the filling of one of the fluvial channels in the upper part of the unit, from which the floodplain *vs.* channel deposit ratio increases significantly.

Recent studies revealed that the Chorrillo Formation strata carries a diverse faunal assemblage including terrestrial and freshwater snails, anurans, fishes, turtles, snakes, sauropods, theropods, ornithischians, and mammals (e.g., Novas et al., 2019; Rozadilla et al., 2021; Chimento et al., 2020, 2021, Aranciaga Rolando et al., 2022). Moreover, plants have also been described in the unit, including conifer wood, Nymphaeaceae, eudicot and monocot leaf impressions, pollen and spores, and fungal remains (Novas et al., 2019; Moyano Paz et al., 2022a; Vera et al., 2022).

In order to evaluate the vertical distribution of the paleosols, we informally divided the unit into three sections: lower (up to 160 m in Fig. 2), middle (up to 450 m in Fig. 2), and upper (up to 515 m in Fig. 2).

2.1.1. The lower section of the Chorrillo Formation

This section is integrated by channels of 4–6 m-thick and up to 100 m of lateral continuity (width/thickness ratio = 16–25) that are characterized by complex gravelly narrow sheet bodies, and by thick fine-grained deposits of the distal floodplain, and thin dark fine-grained deposits of swamp or pond settings into the floodplain (Moyano-Paz et al., 2022a).

Four fossiliferous levels including 1) the fossil wood *Podocarpoxylon dusenii* Kraüsel (Novas et al., 2019), and palynofloras dominated by psilate spores related with the fern families Cyatheaceae, Dicksoniaceae, Dipteridaceae or Matoniaceae, subordinate bisaccate and trisaccate pollen grains of the conifer family Podocarpaceae, and angiosperm pollen grains where is abundant the species *Peninsulapollis gilli* related to Proteales (Novas et al., 2019), 2) crocodile remains, 3) the sauropod *Nullotitan glaciaris* and the avian *Kookne yeutensis*, and 4) plant debris and *Podocarpoxylon dusenii* wood occurs in this section (see Fig. 2) (Novas et al., 2019; Rozadilla et al., 2021; Moyano-Paz et al., 2022a). Palynological assemblages studied by Perez Loinaze et al. (2023) are dominated by the pollen genus Classopollis belonging to the extinct conifer family Cheirolepidiaceae. Subordinate elements are psilate spores related with the fern families Cyatheaceae, Dicksoniaceae, Dipteridaceae or Matoniaceae, and megaspores of Salviniales, together with spores of bryophytes and lycopodialeans. Among angiosperms are identified Gunnerales (*Tricolpites reticulatus),* Liliales (*Liliacidites variegatus*) and Areacaceae (*Arecipites minutiscabratus*).

2.1.2. The middle section of the Chorrillo Formation

In these section, fluvial channels are up to 6 m-thick and 100–200 m of lateral continuity represented mainly by complex sandy narrow sheets (i.e., width/thickness ratio =

15–100 *sensu* Gibling, 2006) intercalated into the floodplain deposits, which is integrated by thick fine-grained deposits and thin dark fine-grained deposits of swamps/ponds. Sandstone lobes of crevasse splay closely related to floodplain deposits are also present in this section (Moyano-Paz et al., 2022a).

The two megafloristic levels described by Vera et al. (2022) are developed in pond deposits of this section of the unit (i.e., megafloristic 1 and megafloristic 2) (see Fig. 2). Palynological assemblages recovered from different levels of this section (Perez Loinaze et al., 2023) are somewhat similar to the ones present in the lower section. Major differences are an increase in abundance of aquatic ferns (Marsileaceae and Salviniaceae), an increase in abundance of Araucariaceae and Podocarpaceae, as well as pteridosperms (*Vitreisporites*) and *Cycadopites*, pollen with diverse affinities (Cicadales, Bennettitales or Ginkoales). Among angiosperms, Arecaceae and Liliales become more abundant. Additionally, four vertebrate fossiliferous intervals including 1) *Magallanodon* Site, 2) *Isasicursor* 1 Site, 3) a level containing the Megaraptoridae *Maip macrothorax* and 4) a level with sauropod remains occurs in this section (see Fig. 2) (Novas et al., 2019; Chimento et al., 2020, 2021; Aranciaga-Rolando et al., 2022; Moyano-Paz et al., 2022a).

2.1.3. The upper section of the Chorrillo Formation

This section is widely dominated by thick fine-grained deposits of the distal floodplain with very scarce thin dark fine-grained deposits of the swamp/pond environment. Such deposits are interbedded with fluvial channels, which are up to 5 m-thick and 300–1000 m of lateral continuity (width/thickness ratio = 60–200), represented by complex sandy narrow sheets to broad sheets (*sensu* Gibling, 2006), and crevasse splay deposits (Moyano-

Paz et al., 2022a). The top of the unit is defined by the appearance of the marine deposits of the Calafate Formation.

A fossiliferous level known as *Isasicursor* 2 Site develops in swamp/pond deposits of this section of the Chorrillo Formation (see Fig. 2). Palynological assemblages recovered from this section are presented below.

3. Materials and methods

The Chorrillo Formation paleosols were studied at the cliffs located in the vicinity of the Estancia La Anita locality (50°30’48.80’’ S, 72°33’46.82’’W), where the entire succession is exposed, and were a complete and detailed sedimentary section was measured by Moyano Paz et al. (2022) (Fig. 1). Here, we performed a combined study using macro- and micromorphology, and clay mineralogy, which is a powerful tool for understanding the environmental and climatic conditions of fossil fluvial sedimentary successions bearing paleosols (e.g., Raigemborn et al., 2018, 2022; Varela et al., 2018; Basilici et al., 2022). Also, selected soil horizons and fine-grained beds without pedogenesis of the upper section of the Chorrillo Formation were sampled for palynology (Fig. 2).

3.1. Macro and micromorphology

At the study area we produce detailed paleopedological logs following Retallack (2001) and Tabor et al. (2017). Paleosols were identified in outcrop based on macroscopic pedofeatures, such as structure, mottles, nodules, color, slickensides, and rhizoliths (e.g., Retallack, 1988, 2001). Colors were described according to the Munsell notation (Munsell Color, 2013). In paleosol horizons, thickness, distinctness and topography, mineral composition, mean grain size, paleosol structure, type of nodules, and evidence of bioturbation were described (e.g., Soil Survey Staff, 1999, 2015; Retallack, 2001; Schoeneberger et al., 2012). Horizon designations were based on observable pedogenic features in the field (Soil Survey Staff, 1999, 2015), and supported later by thin-section detailing. Macro-pedofeatures are listed in Table 1.

Paleosol horizons were sampled for micromorphological studies in order to provide more detailed information; these studies were carried out with a Nikon Eclipse E-200 polarizing microscope (Centro de Investigaciones Geológicas, La Plata, Argentina). Thin sections of oriented samples from each horizon were analyzed and interpreted according to Bullock et al. (1985), Stoops (2003) and Stoops et al. (2010, 2018), and are listed in Table 1. . Pedogenic macro and micromorphological redoximorphic features were described following Lindbo et al. (2010) and Vepraskas (2015).

Paleosol classification was based on macro- and micromorphological features, mineralogy, and mineralogical composition recognized in the constituent horizons, through a comparison with the USDA soil taxonomy (Soil Survey Staff, 1999, 2015) and with the paleosol classification of Mack et al. (1993).

3.2. X-Ray Diffraction

Bulk-rock and clay mineralogy of the paleosols were determined from X-ray diffraction (XRD) pattern (Table 2). Analyses were run on a PANalytical X'Pert PRO diffractometer (Centro de Investigaciones Geológicas, La Plata, Argentina), using Cu radiation ($K\alpha$=1.5 Å) and a Ni filter, and generation settings of 40 kV and 40 mA. Routine air-dried mounts were run between 2 and 32 °2θ at a scan speed of 2 °2θ/min. Samples were ethylene glycol-solvated without saturation pre-treatment and heated to 550 °C, and they were run from 2 to 27 °2θ and 3-15 °2θ, respectively, at a scan speed of 2 °2θ/min. The methodology used for sample preparation follows Brown and Brindley (1980).

Selected matrix paleosol samples, nodules and rhizoliths from the designated pedotypes were collected to determine clay and non-clay mineral composition. Identification of clay and non-clay minerals was based on their characteristic reflections in the XRD patterns (Moore and Reynolds, 1997). The estimation of the mineralogical components is classified according to the following abundances: traces (<1%); very scarce (1–5%); scarce (5–15%); moderate (15–30%); abundant (30–50%), very abundant (50–80%), and extremely abundant (>80%). Semi-quantification of the relative percentages of clay minerals was based on the peak area method on glycolated samples by applying empirical factors (Schultz, 1964; Biscaye, 1965; Moore and Reynolds, 1997; Raigemborn et al., 2014).

3.3. Palynological study

The logged profile of the Chorrillo Formation was sampled for palynology. A total of 23 fertile samples were analyzed, including the ones presented in Novas et al. (2019), Vera et al. (2022) and Perez Loinaze et al. (2023), as well as new samples from the upper section of the unit present in this study (see below and Fig. 2). The samples were processed using standard palynological techniques for extraction and concentration of palynomorphs (Phipps and Playford, 1984). The organic residues were sieved using 20 mm and 10 mm mesh and mounted in permanent slides following the procedures of Noetinger et al. (2017). Palynomorphs were examined with an Olympus BX-51 microscope.

4. Results

4.1. Paleopedological study

Based on prevalent pedogenic features, five different pedotypes were defined throughout the Chorrillo Formation succession following the criteria of Retallack (1994, 1998), in which the name is referring to geographic localities in the vicinity of the study area. Pedotypes are described in the order of their decreasing relative abundance (abundance in thickness) in the stratigraphic section. Detailed macro- and micromorphological descriptions, mineralogy and dominance of pedogenic processes of each pedotype are reported in Tables 1 and 2, and Figures 3 to 7.

Although soil classification is based on characteristics that can be observable on modern soils, classification of paleosols can be complicated because some of such characteristics are not detectable in paleosols. The classification of the pedotypes of the Chorrillo Formation is based on recognition of macromorphology, diagnostic horizons, and micromorphology, which can be preserved on long timescales (e.g., Mack et al., 1993; Retallack, 1993; Soil Survey Staff, 1999, 2014).

All the pedotypes of the Chorrillo Formation have parent material in distal floodplain facies associations (i.e., massive mudstone–siltstone deposits, Fm facies following Moyano Paz et at., 2022), except Centinela River pedotype whose parent material is in swamp/pond facies associations (thin-laminated claystone–mudstone deposits, Fl facies following Moyano Paz et at., 2022) (Table 1). X-ray diffraction analyses of non-pedogenized both Fm and Fl facies indicate that smectite is the main component within the clay fraction.

4.1.1. Argentino Lake pedotype

Description: this pedotype (50% of the all paleosol thickness in the measured section) is the most abundant pedotype throughout the studied section (Fig. 2 and 3), and it is represented by the vertical stacking of well-defined ABss and Bssg horizons with diffuse distinctness and smooth topography (Fig 3A–G, Table 1). Micromorphological analysis confirmed the presence of ABss horizons and Bssg horizons.

The ABss is a reddish black to gray (10R 2.5/1, 5Y 5/1) mudstone horizon that is 0.2 to 0.4 m thick. Its lower horizon is a Bssg horizon; the vertical transitions are diffuse. Macroscopic features include strong brown (7.5YR 5/8) mm-diameter rhizoliths, gley color (5GY 8/1 light greenish gray) rhizohaloes, and slickensides that divide medium–coarse angular blocky or wedge-shaped peds (10–30 mm in diameter). The coarse fraction (>20 μ) of the groundmass includes quartz and plagioclases, while the micromass (<20 μ) is mainly formed of clays impregnated with of Fe/Mn oxides. The c/f (coarse/fine) related distribution pattern is open to double spaced porphyric. The micromass is characterized by stipple-speckled to incipient cross-striated b-fabric (Fig. 3E). Microfeatures of ABss horizons include angular–subangular blocky and wedge-shaped microstructure defined by planar voids, redoximorphic features such as Fe-nodules and depletion zones, and pedorelicts. The mineral components identified by XRD in ABss horizons are, in decreasing order of abundance, quartz, clays, plagioclases and feldspars (Table 2). The clay mineral association (Fig. 3B) is dominated by extremely abundant–very abundant (80–100%) smectite, (5–10%) illite and/or chlorite, and (5%) mixed layers of illite-smectite and/or kaolinite. Smectite presents well defined peaks on XRD diagrams, which varied from sharp to broad suggesting well to poorly crystallized smectites.

The Bssg horizon is very dusky red and dark gray to gray (2.5YR 2.5/2, 5Y 4/1, 10YR 5/1) mudstone horizon that is 0.2–0.6 m thick. The most typical macromorphological features are slickensides that defined fine–coarse subangular to angular blocky peds and wedge-shaped peds (0.5–50 mm in diameter; Fig. 3C), millimeter gray (2.5Y 6/1) and black (Gley 1 2.5/N) rhizoliths, gley (pale green 5G8/2 and dark gray Gley 1 4/N) rhizohaloes, and olive yellow (5Y 6/8), light greenish gray (5GY 8/1) and very dark brown (7.5YR 2.5/3) mottles (Fig. 3D). The coarse fraction (>20 µ) of the groundmass includes quartz and plagioclases. The micromass (<20 µ) is mainly formed of clays impregnated with of Fe/Mn oxides. The c/f (coarse/fine) related distribution pattern is open to double spaced porphyric. The micromass is characterized by stipple-speckled and cross- and parallel-striated b-fabric (Fig. 3F). Microfeatures of Bssg horizons include blocky microstructure defined by planar voids, Fe-nodules and -mottles and depletion zones (Fig. 3G). The mineral components identified by XRD in Bssg horizons of the Argentino Lake pedotype are, in decreasing order of abundance, clays/quartz, plagioclases and k-feldspars (Table 2). The clay mineralogy of the Bssg horizons (Fig. 3B) is dominated by extremely abundant to very abundant (60–100%) smectite, scarce–moderate (5–20%) illite and/or chlorite, and very scarce–scarce (5%) mixed layers of illite-smectite and/or kaolinite. Smectite shows mainly broad and well defined peaks on XRD diagrams that indicate poorly crystallized smectites. However, sharp peaks suggesting well crystallized ones were also detected.

Interpretation and classification: the Argentino Lake pedotype shows no clear differentiation between the soil profiles and there are overlapping features, especially in horizons A and B, giving transitional horizons of ABss type resulting from the mixing and pedoturbation process indicating that this pedotyope is a moderately developed paleosol.

The dominance of smectite clays (>60%) and the high content of clay in the groundmass is in correlation with the abundance of vertic features (see Table 1), which indicate seasonal shrink-swell processes (e.g., Ahmad, 1983; Ahmad et al., 1996;

Coulombe et al., 1996; Mermut et al., 1996; Retallack, 2001). Redoximorphic features including both concentration or impregnative, and depletion features (see Table 1) also indicate seasonal waterlogged drainage conditions, possibly enhanced by the ability of smectites to retain water (e.g. Retallack, 2001; Raigemborn et al., 2018a; Varela et al., 2018, 2021; Lizzoli et al., 2021). The presence of rhizoliths is evidence of bioturbation. Thus, we interpret that the main pedogenic processes that affected this paleosol were, in decreasing order of importance, vertization, hydromorphism and bioturbation (Table 1). Gley colors and low chroma values less than 2 and inclusive <3, could be due to the lack of free iron and poor-drainage conditions (e.g., Ashley et al., 2013; Kovda, 2020).

Soils with vertic and redoximorphic features are usually associated with a depressed topography with a relatively high watertable and/or impeded drainage conditions being waterlogged during a part of the year (e.g., Soil Survey Staff, 1999; Imbellone et al., 2009). The high content of clay and of smectite as clay mineral in the groundmass, the fine-grained of the matrix, the presence of slickensides, and the occurrence of wedge-shaped peds are features that match with modern Vertisols (Buol et al., 2011; Soil Survey Staff, 2014; Basilici et al., 2022). Other features of this pedotype such as a heterogeneous groundmass, porphyric c/f related distribution, and stipple-speckled and striated b-fabric, are also compatible with modern Vertisols (Kovda and Mermut, 2010, 2018). However, Argentino Lake pedotype present redoximorphic features linked to the fact that these soils were exposed to alternating oxidation and reduction conditions. Consequently, and according to the abundance of vertic and redoximorphic features, this pedotype can be classified as a hydromorphic Vertisol-like paleosols (i.e., Aquerts following Soil Survey Staff, 1999, 2014), and as gleyed Vertisols following Mack et al. (1993).

4.1.2. Perito Moreno Glacier pedotype

Description: this pedotype (20% of the all paleosol thickness in the measured section) is only recorded in the middle section of the unit (Figs. 2 and 4), and it is represented by the vertical stacking of not well-defined ABssg, Bssk and Ck horizons with diffuse distinctness and smooth topography (Fig. 4A–G; Table 1). Micromorphological analysis confirmed the presence of ABssg horizons Bssk horizons and C horizons.

The ABssg is a very dusky red (2.5YR 2.5/2) silty horizon that is 0.3 to 0.4 m thick. Its lower horizon is a Bssk horizon; the vertical transitions are diffuse. Macroscopic features include rhizoliths (7.5YR 5/8 strong brown, mm-diameter), gley color rhizohaloes (5GY 8/1 light greenish gray) and mottles (Gley 1 2.5/N black and light greenish gray), Fe-nodules (2.5YR 2.5/2 very dusky red, cm-diameter), and slickensides that divide fine–coarse angular blocky peds (5–50 mm in diameter). The coarse fraction (>20 μ) of the groundmass includes quartz and plagioclases, while the micromass (<20 μ) is mainly formed of clays impregnated with of Fe/Mn oxides. The c/f (coarse/fine) related distribution pattern is open to double spaced porphyric. The micromass is characterized by stipple-speckled to incipient cross-striated b-fabric. Microfeatures of ABssg horizons include angular–subangular blocky and wedge-shaped microstructure defined by planar voids, Fe-nodules, depletion zones, and pedorelicts. The mineral components identified by XRD in ABssg horizons of the P2 are quartz, plagioclases, clays, k-feldspars, and calcite (Table 2). The clay mineral association (Fig. 4B) is dominated by very abundant–extremely abundant (65–80%) smectite, scarce to moderate (10–30%) illite, scarce (5–10%) mixed layer of illite-smectite, and up to scarce (<15%) chlorite. Smectite presents broad and well defined peaks on XRD diagrams that indicate poor degree of crystallization.

The Bssk is a dusky red and dark reddish gray (10R 3/2, 7.5R 4/1) silty horizon that is 0.4 to 0.7 m thick. Its lower horizon is a Ck horizon; the vertical transitions are diffuse. Macroscopic features include rhizoliths (Gley 1 2.5/N black, mm-diameter), gley colors rhizohaloes and mottles (5GY 8/1 light greenish gray) (Fig. 4D), and slickensides that divide very fine–fine angular blocky peds (<5–10 mm in diameter). Carbonate-nodules are the distinctive feature of the Bssk horizon (Fig. 4C). The nodules are mainly isolated, subspherical in shape and with diameters between 20 and 150 mm. In a lesser extent, nodules are coalescent with a maximum diameter of 300 mm. The colors of the nodules are weak red (10R 4/2) to light brown (7.5YR 6/4), and externally they are smooth or present a network of cracks with a reticular arrangement. Carbonate nodules of this pedotype are equivalent to the stage II of the soil carbonate development of Machette (1985), Gile et al. (1996) and Birkeland (1999). The coarse fraction (>20 μ) of the groundmass of the matrix of the Bssk horizons includes quartz and plagioclases, while the micromass (<20 μ) is mainly formed of clays impregnated with of Fe/Mn oxides, and minority calcite. The c/f (coarse/fine) related distribution pattern is open to double spaced porphyric (Fig. 4G). The micromass is characterized by cross- and grano-striated b-fabric. Microfeatures of Bssk horizons include angular blocky and wedge-shaped microstructure defined by planar voids, carbonate-nodules, depletion zones (Fig. 4F), and pedorelicts. Micromorphologically, the groundmass of the carbonate-nodules is composed of micritic carbonate with impregnated Fe/Mn-zones (nodules and hypocoatings). Carbonate-crescent coatings, floating-grains with calcite-bladed coronas, and vermiform voids and cracks infilled with microsparite are also present in the groundmass of the nodules (Fig. 4E). The mineral components identified by XRD in Bssk horizons of the Perito Moreno Glacier pedotype are, in decreasing order of abundance, quartz, plagioclases, clays and k-feldspars (Table 2). The clay mineral association (Fig. 4B) is dominated by very abundant to extremely abundant (60–95%) smectite, scarce to moderate (5–20%) illite, very scarce (<5%) mixed layers of illite-smectite and chlorite, and exceptionally moderate (<15) kaolinite. Smectite peaks on XRD diagrams are broad and well-defined suggesting poorly crystallized smectites. Meanwhile, mineral components identified by XRD in nodules of the Bssk horizons of this pedotype are, in decreasing order of abundance, calcite, quartz, clays, plagioclases and feldspars (Table 2). The clay mineral association (Fig. 4B) is dominated by extremely abundant–very abundant (60–100%) smectite, scarce–moderate (5–15%) illite and kaolinite, scarce (5–10%) chlorite, and very scarce–scarce (5%) mixed layers of illite-smectite. Smectite shows broad and well defined peaks on XRD diagrams that indicate poorly crystallized smectites.

The Ck horizon is a weak red (10R 4/2) silty horizon that is 0.6 m thick. The horizon is massive and includes gley mottles (5GY 8/1 light greenish gray) and powdery carbonate.

Interpretation and classification: similarly to Argentino Lake pedotype, Perito Moreno Glacier pedotype shows no clear differentiation especially in horizons A and B with overlapping features, giving transitional horizons of ABssg type resulting from the mixing and pedoturbation process. Also, the moderate degree of development of pedofeatures attests to limited time of soil formation, indicating that this pedotype is a moderately developed paleosol.

The occurrence of carbonate macro and microfeatures indicates calcification process. Particularly, micritic groundmass, micritic coatings and vermiform voids are Beta-microfabrics that are associated to organic processes and that are present in biogenic calcretes. These allow us to interpreted carbonate nodules as pedogenic nodules induced by biological activity (e.g., Alonso-Zarza et al., 1998). The network of cracks with a reticular arrangement into the surface of carbonate nodules can be related to root penetration, are interpreted as desiccation cracks, but also with desiccation of the fine-grained host substrate during formation (Ashley et al., 2013; Sacristán-Horcajada et el., 2016; Raigemborn et al., 2018b). This last, together with floating-grains, calcite-bladed coronas and cements infilling cracks are Alpha-microfabrics, suggest inorganic processes (e.g., Alonso-Zarza et al., 1998; Raigemborn et al., 2018b). Thus, the combination of both types of fabrics is considered indicative of multiple calcretization phases (e.g., Adamson et al., 2015; Raigemborn et al., 2018b). The dominance of smectite clays (>60%) and the abundance of vertic features (see Table 1) indicate seasonal shrink-swell processes (e.g., Ahmad, 1983; Ahmad et al., 1996; Coulombe et al., 1996; Mermut et al., 1996; Retallack, 2001). Redoximorphic features (see Table 1) indicate fluctuating soil moisture levels (e.g., Kraus and Hasiotis, 2006; Ashley et al., 2013; Raigemborn et al., 2018a), while rhizoliths indicate bioturbation. The carbonate pedofeatures indicates that the horizon was at least moderately well-drained and oxidized (e.g., Kraus and Hasiotis, 2006), but the occurrence of mottles, Fe-nodules, rhizohaloes, depleted zones and Fe-Mn impregnations attest to fluctuating watertable. The intergrowth of Fe-Mn oxides and carbonate in the nodules indicate alternating oxidizing and reducing conditions within the soil (e.g., Kraus and Aslan, 1993; Therrien et al., 2009; Raigemborn et al., 2018b). Perito Moreno Glacier pedotype also show features linked to formation under alternating wet and dry periods. The abundance of redoximorphic features at the surficial horizon indicates that soils were saturated for a prolonged period of time due to the fact that the water infiltration was retained in the solum. However, the scarcity of redoximorphic features at the subsurficial horizons of the profile together with the carbonate features and the coarser grained texture attest to that the watertable rarely saturated these soils for extended periods of time (e.g., Therrien et al., 2009). Thus, we interpret that this pedotype probably formed under imperfectly- to moderately well-drained floodplains characterized by seasonal fluctuations of the watertable. The main pedogenic processes that affected this paleosol were, in decreasing order of importance, vertization, calcification, hydromorphism, and bioturbation (Table 1).

Likely Argentino Lake pedotype, Perito Moreno Glacier pedotype can be classified as Vertisol-like paleosols (Soil Survey Staff, 1999, 2014). However, the occurrence of a Bssk and Ck horizons with pedogenic carbonate features allow us to classify this pedotype as calcic Vertisols (Soil Survey Staff, 1999, 2014), or as vertic Calcisols following Mack et al. (1993).

4.1.3. Anita Farm pedotype

Description: this pedotype (16% of the all paleosol thickness in the measured section) is recorded in the lower and middle part of the unit (Figs. 2 and 5), and it is represented by the vertical stacking of well-defined Bssg and C horizons with diffuse distinctness and smooth topography (Table 1). Micromorphological analysis confirmed the presence of well-developed Bssg horizons (Fig. 5A–G).

The Bssg horizon is a gray and very dark bluish gray (5Y 6/1, Gley 2 3/5PB) mudstone horizon that is 0.2 to 0.6 m thick (Fig. 5C). Its lower horizon is a C horizon; the vertical transitions are diffuse. Macroscopic features include yellow and light greenish gray (5Y 7/6 and 5GY 8/1) mottles (Fig. 5D), weak red (5R 4/2) Fe-nodules of 5 to 15 mm-diameter, and strong brown and black (7.5YR 5/8 and Gley 1 2.5/N) rhizoliths of millimeter-diameter, some of them with horizontal disposition. Very fine–coarse subangular blocky peds (<5–50 mm in diameter) and diffuse slickensides are present. The coarse fraction (>20 μ) of the groundmass includes quartz, plagioclases and volcanic lithics, while the micromass (<20 µ) is mainly formed of clays impregnated with of Fe/Mn oxides. The c/f (coarse/fine) related distribution pattern is open to single spaced porphyric. The micromass is characterized by incipient grano-striated b-fabric (Fig. 5E). Microfeatures of Bssg horizons include angular–subangular blocky microstructure defined by planar voids, channels, Fe-nodules and -hypocoatings, and depletion zones (Fig. 5F–G). The mineral components identified by XRD in Bssg horizons of this pedotype are in decreasing order of abundance quartz, clays, plagioclases and k-feldspars (Table 2). The clay mineral association (Fig. 5B) is dominated by extremely abundant (80–100%) smectite, and scarce (5–10%) illite, mixed layer of illite-smectite and/or kaolinite. Smectite peaks on XRD diagrams are relatively sharp and well defined suggesting relatively good crystallized smectites. Also, broad peaks were detected, which indicate poorly crystallized smectites.

The C horizon is a massive black (Gley 1 2.5/N) muddy horizon that is 0.4 m thick. The only macroscopic feature recognized are light greenish gray (5Y 7/6) mottles.

Interpretation and classification: the thinner profile of the Anita Farm pedotype relative to Argentino Lake and Perito Moreno Glacier pedotypes indicates that the this pedotype is more poorly developed. The dominance of redoximorphic features in Anita Farm pedotype (see Table 1) indicate fluctuating soil moisture levels (e.g., Kraus and Hasiotis, 2006; Ashley et al., 2013). Particularly, gleyed matrix as those of this pedotype indicate extended periods of water saturation (e.g., Therrien et al., 2009). Abundant smectite (>80%) and the occurrence of vertic features (see Table 1) indicate seasonal shrink-swell processes (e.g., Ahmad, 1983; Ahmad et al., 1996; Coulombe et al., 1996; Mermut et al., 1996; Retallack, 2001), while rhizoliths and micro-channel voids indicate bioturbation. Thus, the main pedogenic processes that took place in this pedotype are, in decreasing order of importance, hydromorphism, vertization and bioturbation (Table 1).

In Anita farm pedotype, erosional surfaces and coarse-grained deposits overlying the top of the Bssg horizons suggest that the A horizon was probably eroded. However, in the cases in which paleosol profiles are not marked by deposits or erosional surfaces, it is possible that the A horizons could be superposed by and confused with the B horizon due to the cumulative character of paleosols (e.g., Marriott and Wright, 1993; Basilici et al., 2022). Moderately well-defined horizons with slightly structured B horizon, poor developed ped structure, and evidence of pedoturbation (rhizoliths, mottles, nodules) are evidences of limited pedogenesis. Fe-nodules and mottles present in Bssg horizons of the Anita Farm pedotype may indicate former water table positions in which pH and Eh conditions change abruptly due to fluctuating watertables (e.g., Vepraskas, 1992, 1994, 2015; Retallack, 2001). Particularly, the presence of Fe-mottles suggests that this pedotype may have been slightly better drained than the Centinela River pedotype (see below) (e.g., Therrien et al., 2009). Moreover, horizontal rhizoliths in Bssg horizons represent a typical adaptation of plants in order to provide anchorage in partially waterlogged zones (Kraus and Hasiotis, 2006; Ashley et al., 2013). Thus, this pedotype is interpreted as a weak developed hydromorphic paleosol with vertic features that formed in poorly-drained environments with a fluctuating watertable. Although weakly developed soils can be classified as Inceptisols (Soil Survey Staff, 1999, 2014), this type of soil is ruled out because of the lack of a subsurface cambic horizon (Bw) and by the occurrence of diagnostic features of other soil orders (e.g., vertic features). Thus, similarly to Argentino Lake pedotype, the Anita farm pedotype can be comparable to modern hydromorphic Vertisols (Soil Survey Staff, 1999, 2014), and it may be classified as a hydromorphic Vertisol-like paleosol, or as a gleyed Vertisol following Mack et al. (1993). Despite both pedotypes being identified as hydromorphic Vertisols, the Anita Farm pedotype, suggest a lower degree of development than the Argentino Lake pedotype. Therefore, the here interpreted pedotype could represent fossil hydromorphic Vertisols with a poor degree of development.

4.1.4. Centinela River pedotype

Description: this pedotype (10% of the all paleosol thickness in the measured section) is recorded exclusively in the middle part of the unit (Figs. 2 and 6), and it is represented by the vertical stacking of well-defined Oa, ABg and Bg horizons with diffuse distinctness and smooth topography (Table 1). Micromorphological analysis confirmed the presence of well-developed Oa, ABg horizons, and Bg horizons (Fig. 6A–G).

The Oa horizon is a dark gray and dark grayish olive (2.5Y 4/1, 5GY 4/2) muddy horizon that is 0.3 m thick. Its lower horizon is an ABg horizon; the vertical transitions are sharp. Macroscopic features of Oa horizon (Fig. 6C) includes black (Gley 1 2.5/N) carbonized organic matter, remains of leaves and fiber, all of them with different degree of carbonization, black rhizoliths (Gley 1 2.5/N) of millimeter-diameter, reddish black rhizohaloes (10R 2.5/1), and very coarse platy peds (>10 mm thick). The coarse fraction (>20 μ) of the groundmass includes carbonaceous remains (cells and tissues), carbonized plant fragments (Fig. 6E), quartz and plagioclases, while the micromass (<20 μ) is mainly formed of clays. The c/f (coarse/fine) related distribution pattern is single- to close-spaced porphyric. The micromass is characterized by speckled b-fabric, and in less proportion by grano-striated b-fabric. Microfeatures of Oa horizons include platy to subangular blocky microstructure defined by channels and chambers, and Fe-nodules and -hypocoatings. The mineral components identified by XRD in Oa horizons of this pedotype are, in decreasing order of abundance, quartz, clays, plagioclases and k-feldspars (Table 2). The clay mineral association (Fig. 6B) is dominated by very abundant (65–80 %) smectite, scarce to moderate chlorite (10–20%), and scarce (10%) illite. Smectite shows relatively sharp and well defined peaks on XRD diagrams, which suggest well crystallized smectites.

The ABg horizon is a grayish brown (2.5Y 5/2) mudstone horizon that is 0.4 m thick. Its lower horizon is a Bg horizon; the vertical transitions are diffuse. Macroscopic features include fine black (Gley 1 2.5/N) rhizoliths and coarse yellowish red (5YR 5/8) rhizoliths (5–15 mm; Fig. 6D), yellowish red mottles (5YR 5/8), and fine to medium subangular blocky peds (5–20 mm thick). The coarse fraction (>20 μ) of the groundmass includes quartz and plagioclases, while the micromass (<20 μ) is mainly formed of clays impregnated with of Fe/Mn oxides. The c/f (coarse/fine) related distribution pattern is single- to double-spaced porphyric. The b-fabric of the micromass is undifferentiated. Microfeatures of ABg horizons include subangular blocky microstructure defined by channels and chambers (Fig. 6F), and Fe-nodules and -coatings. The mineral components identified by XRD in ABg horizons of this pedotype are, in decreasing order of abundance, quartz, clays, plagioclases and k-feldspars (Table 2). The clay mineral association (Fig. 6B) is dominated by extremely abundant (85%) smectite and scarce–moderate illite (15%). Smectite in ABg horizon shows relatively sharp and well defined peaks on XRD diagrams, suggesting well crystallized smectites.

The Bg horizon is a brown and olive gray (10YR 5/3, 5Y 4/2) mudstone horizon that is 0.4 m thick. Macroscopic features include rhizoliths (yellowish red, mm-diameter), mottles (yellowish red), carbonaceous remains, slickensides, and medium to coarse subangular blocky peds (10–50 mm thick). The coarse fraction (>20 μ) of the groundmass includes quartz and plagioclases, while the micromass (<20 μ) is mainly formed of clays impregnated with of Fe/Mn oxides. The c/f (coarse/fine) related distribution pattern is single- to close-spaced porphyric. The micromass is characterized by incipient cross-striated b-fabric. Microfeatures of Bg horizons include angular blocky and wedge-shaped microstructure defined by planar voids, Fe-nodules, and depletion zones (Fig. 6G). The mineral components identified by XRD in Bg horizons of the Centinela River pedotype are, in decreasing order of abundance, quartz, clays, plagioclases and k-feldspars (Table 2). The clay mineral association (Fig. 6B) is dominated by extremely abundant smectite (90–100%) and scarce chlorite (10%). Smectite presents relatively sharp and well defined peaks on XRD diagrams that indicate well crystallized smectites.

Interpretation and classification: the Centinela River pedotype presents a relatively well developed horizon sequence (Oa-ABg-Bg profiles) and thick profiles indicating that this pedotype is a moderately developed paleosol. The high content of organic matter and floral remains suggest that vegetation grew in proximities to the ponds of the swamp setting, probably in the margins of the ponds. Organic matter probably derived from the in situ accumulation of plant material (e.g., Tabor et al., 2017). The preservation of organic matter indicates anoxic and reducing conditions resulting from high watertables as typically occurs in hydromorphic soils (e.g., Wright et al., 2000; Kraus and Hasiotis, 2006; Raigemborn et al., 2018b). This pedotype is dominated by redoximorphic features such as gleyed matrix, which are related to poor drainage conditions and extended periods of water saturation due to high nonfluctuating watertable (e.g., Therrien et al., 2009; Lindbo et al., 2010; Vepraskas. 2015; Vepraskas and Craft, 2016; Vepraskas et al., 2018). Abundant smectite (>65%) also attest to waterlogged conditions (e.g., Varela et al., 2018). However, the occurrence of incipient vertic features mainly in the Bg horizon of this pedotype (see Table 1) indicate shrink-swell processes (e.g., Ahmad, 1983; Ahmad et al., 1996; Coulombe et al., 1996; Mermut et al., 1996; Retallack, 2001). Rhizoliths, micro-channel voids and micro-chambers indicate bioturbation. The abundance of macro- and micromorphological features testified that subaerial exposure was relatively long, and the main pedogenic processes that took place in this pedotype are, in decreasing order of importance, hydromorphism, bioturbation and vertization (Table 1). Thus, Centinela River pedotype is interpreted as a moderately developed paleosol that formed in very poorly-drained environments.

The occurrence of a histic epipedon (Oa horizon), abundant carbonized plant fragments and carbonaceous material, and gley mottles of this pedotype resemble to modern Histosols (Soil Survey Staff, 1999, 2014). This type of soil occurs in topographically low areas with very poor drainage conditions. Although this soils are defined by the presence of a histic and/or folisitc epipedon, which is recognized for a content of organic carbon of at least 8% (Soil Survey Staff, 1999, 2014), fossil Histosols are defined as paleosols that contained a layer of concentrated organic matter that accumulated in situ (e.g., Mack et al., 1993; Kahmann et al 2008; Tabor et al., 2017). Paleosols typically have significantly less organic matter than their modern equivalents due to efficient biotic decomposition as well as burial dissolution (Retallack, 1991; Sheldon, 2003). Thus, the Centinela River pedotype may be classified as a Histosol-like paleosol, or as a Histosol following Mack et al. (1993).

4.1.5. Chorrillo Malo Farm pedotype

Description: this pedotype (4% of the all paleosol thickness in the measured section) is recorded exclusively in the uppermost part of the unit (Figs. 2 and 7), and it is represented by the vertical stacking of Bss horizons (Table 1). The micromorphological analysis of this pedotype confirmed the presence of Bss horizons (Fig. 7A–E).

The Bss horizon is a weak red (10R 4/3) siltstone–mudstone horizon that is 0.5 m thick. Its lower horizon is a C horizon; the vertical transitions are diffuse. Macroscopic features include black (Gley 1 2.5/N) rhizoliths of mm-diameter, light greenish gray (5GY 8/1) rhizohaloes, slickensides, and incipient coarse subangular–angular peds (20–30 mm thick; Fig. 7C). The coarse fraction (>20 μ) of the groundmass includes quartz and plagioclases, while the micromass (<20 μ) is mainly formed of clays impregnated with of Fe/Mn oxides. The c/f (coarse/fine) related distribution pattern is open-spaced porphyric. The micromass is characterized by speckled b-fabric or it is undifferentiated. Microfeatures of Bss horizons include typic Fe- and -clay coatings around voids associated with depletion zones (Fig. 7D–E), subangular blocky microstructure defined by channels, and Fe-nodules. The mineral components identified by XRD in Bss horizons of this pedotype are, in decreasing order of abundance, quartz, clays, plagioclases and k-feldspars (Table 2). The clay mineral association (Fig. 7B) is dominated by very abundant (60%) smectite, moderate–abundant (30%) illite, and very scarce–scarce (5%) chlorite and kaolinite. Smectite of Bss horizon shows relatively good and well defined peaks on XRD diagrams that indicate well crystallized smectites.

The C horizon is a dark red (10R 3/6) siltstone–mudstone horizon that is >0.5 m thick and with massive structure.

Interpretation and classification: this pedotype has moderately well-defined horizonation with slightly structured Bss horizons indicating that soil development is moderate. Evidence of clay accumulation of illuvial origin (argilluviation) is only at microscale. This illuvial clay was probably transported from overlying horizons (A horizon) by rainwater percolating through the soil and preserved as coating when the soil dries. Although the scarce occurrence of this pedofeature is not enough to warrant classification as an argillic horizon (Bt), such feature indicated that the soil must have been part of the vadose zone and responds to well-drained/dry conditions (e.g., Therrien et al., 2009; Ashley et al., 2013). Also, reddish color of the Chorrillo Malo farm pedotype reveals that oxidizing soil conditions were predominant, while the presence of Fe-coatings and -nodules and gley rhizohaloes are evidence of a fluctuating watertable. Rhizoliths and micro-channels attest to bioturbation. The abundance of smectite (60%) clay and the scarce occurrence of vertic and redoximorphic features (Table 1) indicate that seasonal shrink-swell processes and fluctuating soil moisture levels also occurred during its formation. Thus, this pedotype is interpreted as moderately developed paleosols formed on moderately well-drained floodplain settings with a watertable fluctuating during the year. Here, illuviation, bioturbation, vertization and hydromorphism seem to be the main pedogenic processes that took place to this pedotype formation.

Similarly to Anita farm pedotype, the absence of a preserved A horizons suggests that the A horizon was probably eroded or, alternatively, that A horizons could be superposed by and confused with the B horizon due to the cumulative character of paleosols (e.g., Marriott and Wright, 1993; Basilici et al., 2022). Also, likely Argentino Lake and Anita Farm pedotypes, the presence of vertic features in the Chorrillo Malo Farm pedotype are consistent with modern Vertisols (Soil Survey Staff, 1999, 2014; Buol et al., 2011; Schoeneberger et al., 2012). The formation of clay coatings as those of this pedotype, is a common pedogenic phenomenon in seasonally waterlogged clay-rich soils, and was widely recognized in paleo-Vertisols (e.g., Kahmann and Driese, 2008; Pal et al., 2012; Beilinson and Raigemborn, 2013; Licht et al., 2014; Varela et al., 2021). Consequently, this pedotype may be classified as argillic Vertisol-like paleosols (Soil Survey Staff, 2014), and as argillic Vertisols following Mack et al. (1993).

4.2. Palynological study

Palynological assemblages recovered from the upper section of the Chorrillo Formation (see Fig. 2) are characterized by the presence of spores related with lycopsids (e.g., *Densoisporites velatus*), bryophytes (e.g., *Foraminisporis wonthaggiensis*), Salvinialean megaspores, and angiosperm pollen grains of the angiosperm clade Liliales (e.g., *Liliacidites variegatus*). In this section are also abundant cysts of freshwater algae related to Zygnemataceae or Oedogoniaceae (Van Geel and Grenfell, 1996; Zippi, 1998). Pollen of gymnosperms is scarce, unlike what is observed in the lower and middle sections of the unit.

5. Discussion

5.1. The significance of large- and small-scale vertical variations in the paleosols of the Chorrillo Formation

The architectural elements of the Chorrillo Formation in the study area were analyzed by Moyano-Paz et al., (2022a), who defined that it represents a low-gradient fluvial system, comprising of gravelly-sandy fluvial channels, sandy crevasse splays deposits, and ~60% of fine-grained material (massive siltstones and mudstones; Fm facies) of the distal floodplain including swamp/pond settings (laminated claystone–mudstones; Fl facies).

The different pedotypes of the Chorrillo Formation are vertically interspersed throughout the succession. The large-scale or small-frequency stacking of these paleosols and the subtle vertical changes recorded in the architectural elements of the unit (i.e., changes in depositional environments), varying according to the three informal sections within the Chorrillo Formation (Figs. 2 and 8).

Although the relatively low structural dips, extensive slumpings, and the typical badland landscape of the exposures prevent the establishment of mesoscale lateral relationships between each pedotype associated with their relative position within the fluvial environment (i.e., catena following Birkeland, 1999), the occurrence of different paleosols throughout the unit suggests formation under different hydrologic conditions in close stratigraphic proximity (i.e., small-scale or high frequency stacking). This could suggest the existence of multiple landscapes within the floodplain of the Chorrillo Formation.

5.1.1. Lower section of the Chorrillo Formation

Overall, this section is dominated by thick fine-grained deposits of the distal floodplain with the Argentino Lake pedotype (moderately-developed hydromorphic Vertisol-like paleosols), and in less proportion with the Anita Farm pedotype (poorly-developed hydromorphic Vertisol-like paleosols). Thin dark fine-grained deposits comprising swamp/pond settings and very few crevasse splay deposits without pedogenesis are also present in this section of the unit (Moyano-Paz et al., 2022a) (Figs. 2 and 8).

Small-scale or high-frequency vertical variations within this section show sequences of few meters thick where Argentino Lake pedotype is overlain by Anita Farm pedotype, and both paleosols are sharply bounded by channel sandstones. The combination of vertic and redoximorphic features in Vertisols with moderate degree of development attests to seasonality of rainfall and/or waterlogged during a part of the year (seasonal waterlogging). Such conditions could took place on smectite-rich mudstones (Fm facies) of the distal floodplain where slow sediment accumulation occur (e.g., Licht et al., 2013). Meanwhile, the dominance of hydromorphic features in another Vertisol points out to extended periods of water saturation which could be linked to topographically more depressed areas in the distal floodplain. However, both paleosols have the same smectite-rich muddy (Fm facies) parent material suggesting that no significant topographic differences occurred in the floodplain. Thus, one possibility is that difference in drainage reflect both flooding duration on an aggrading floodplain and minor topographic variations, where seasonal fluctuations in the water level enhanced minor topographic differences (e.g., Wright et al., 2000). The poor degree of development of the Anita Farm pedotype can be due to waterlogged conditions, which suppress most of the soil-forming processes (e.g., Ashley et al., 2013).

The vertical stacking of these pedotypes could be related to changes in the position of the main channel and consequently, this vertical change may result of the avulsion of the channel, a common processes of channel abandonment recorded in the Chorrillo Formation (Moyano-Paz et al., 2022a). In this sense, the paths form hydromorphic Vertisols to channel deposits in the lower section of the unit is another record of avulsion mechanism (e.g., Varela et al., 2012), while the vertical stacking of different profiles of this pedotype could be related to a break in sedimentation and pedogenesis and the subsequent formation of a new soil profile. This situation could reflect a "cryptic" avulsion within the fluvial system (i.e., an avulsion that remains hidden within the traditional facies analyses and that only can be revealed by means of paleosols analysis, *sensu* Varela et al., 2012).

Paleobotanical data of this section suggest the presence of vegetation occupying different environments within the low-gradient fluvial system of the Chorrillo Formation. Salviniales (water ferns) were restricted to the water bodies, as swamps and ponds (e.g, Scafati et al., 2009) without soil developed. Surrounding these freshwater bodies, or in other moist places as riverbanks, several spore producing plant groups, as bryophytes, lycopsids, and terrestrial ferns were probably present, along with angiosperms of the Liliales and Gunnerales. The arboreal vegetation present in the assemblage could have grew near river courses (e.g. Proteaceae; Volkheimer et al., 2007), in the upland regions (Podocarpaceae), or in coastal and upland slopes (Hirmeriellaceae; Batten, 1975, Filatoff, 1975) (see Fig. 8).

5.1.2. Middle section of the Chorrillo Formation

The unchannelized deposits of this section are integrated by sandy crevasse splay and thick fine-grained floodplain deposits. In less proportion, thin dark fine-grained deposits of swamp/ponds occur (Moyano-Paz et al., 2022a). The Argentino Lake and the Perito Moreno Glacier (calcic Vertisol-like paleosols) pedotypes dominated this section (Figs. 2 and 8). The Anita Farm, and the Centinela River (Histosol-like paleosols) pedotypes are also present (Figs. 2 and 8).

The small scale vertical stacking of paleosols within this section presents different sequences of few meter-thick. For example, in the lower part a sequence of hydromorphic Vertisols - calcic Vertisols - hydromorphic Vertisols is developed between two crevasse splay deposits(see Fig. 2). Other stacking patterns of the lower part are (1) hydromorphic Vertisols - Histosols sharply bounded by fine-grained floodplain deposits without pedogenesis, (2) hydromorphic Vertisols - Histosols - channel deposits, (3) calcic Vertisols - hydromorphic Vertisols - channel deposits, and (4) stacked hydromorphic Vertisols. Also, Histosols sharply bounded by channel deposits are recorded. Towards the upper part of the section, different hydromorphic Vertisols are associated to calcic Vertisols sharply bounded by channel, or by crevasse splay deposits without pedogenesis. It is important to highlight the lack of pedogenic features in sandy crevasse splay deposits of the Chorrillo Formation (Fig. 2), reflecting the greater proximity of such deposits to the rivers where more frequent floods occur, and the high sedimentation rates and avulsion that would prevent pedogenesis and inhibit soil development (e.g., Kraus, 1999; Yeste et al., 2020).

The Perito Moreno Glacier pedotype is a paleosol with moderate-degree of development that has silt as parent material (Fm facies) and was formed under imperfectly- to moderately well-drained settings characterized by seasonal fluctuations of the watertable. As was mentioned previously, on the basis of the silt-dominated lithology and better drained conditions, this pedotype is related to probably settings in the floodplain in proximity to non-pedogenized crevasse splay deposits (Fig. 8). While, Argentino Lake and Anita Farm pedotypes are related to moderate to poor-drained conditions of the distal floodplain, respectively (Fig. 8), as was mentioned for the lower section of the unit. Besides, the Centinela River pedotype is a moderately developed paleosol in which hydromorphic features are relatively well developed. These features may have formed in distal portions of the floodplain (Fig. 8) where the rate of sedimentation was very low, the grain size of the particles are very fine, and the lowest topographic relief, which in turn favored extended periods of water saturation and very poorly-drained conditions. It is probable that these Histosols have been formed in margins of swamps/ponds (see before), where periods of water saturation were extended due to high non fluctuating watertable. Under waterlogged conditions, soils are in general not well-developed, as is the Centinela River pedotype, because the suppression of most of the soil-forming processes (e.g., Ashley et al., 2013).

Similarly to the lower section of the unit, different stacking patterns of paleosols could reflect changes in the position of the main channel due to avulsion (e.g., Kraus and

Aslan, 1993; Kraus, 1996, 1997). The passage from hydromorphic Vertisols or Histosols to channel deposits also records avulsion process, and the link between stacked paleosols and crevasse splay deposits could be related to the abandoned of the last. The subtle changes between the stacking of hydromorphic Vertisols - calcic Vertisols - hydromorphic Vertisols reflect the vertical superimposition of different paleosols that were developed in close stratigraphic and probably spatial proximity within the floodplain.

The sharp boundary between different paleosols of the middle section could suggest a pause in pedogenesis and the later reestablishment of floodplain aggradation (e.g., Varela et al., 2021). In addition, the stacking of the same paleosol type (i.e., hydromorphic Vertisols in the lower part and calcic Vertisols in the upper part) with the preservation of AB horizons in the profiles could be another example of "cryptic" avulsion as was interpreted for the lower section of the unit.

Throughout the entire section of the Chorrillo Formation, but more frequently within the middle section, there are thin dark fine-grained deposits without pedogenesis (claystone–mudstone Fl facies), interpreted by Moyano-Paz et al. (2022a) as deposited by settling of suspended load in depressions or topographically low areas of the landscape. Such areas were characterized by impeded drainage, producing water-logging, swamp- or pond-like environments. The gray colors of these deposits indicate reducing and anoxic conditions, with organic matter preserved and in such cases, preservation of paleofloristic or paleovertebrate remains (see Figs. 2 and 8). The thin lamination attests to very quiet environments where settling of suspension predominates. Some of these water body were probably very shallow, as was suggested by Vera et al. (2022), based on the recognized aquatic floristic community. These swamp settings probably consisted of (1) ponds without pedogenesis and inhabited by aquatic vegetation (i.e., Nymphaeaceae, *Azzola* spp., Marsileaceae, and Zygnemataceae; Vera et al., 2022), (2) margins colonized by terrestrial components of the vegetation that could have lived in the vicinity of the aquatic community as non-vascular plants, lycopsids, several terrestrial fern groups, terrestrial gymnosperms as Hirmeriellaceae, pteridoperms and Cycadales, Bennettitales or Ginkgoales (*Cycadopites*), as well as some angiosperms as Gunneraceae and Liliales (Vera et al., 2022), where very poorly-drained paleosols with abundant poorly decomposed organic matter (Histosols) developed, and (3) poorly-drained soils (poorly-developed hydromorphic Vertisols) situated topographically slightly higher and/or more distal to ponds, temporally waterlogged and with a fluctuating watertable (see Fig. 8). In fluvial systems with a very low-gradient as those of the Chorrillo Formation, high watertables associated to very fine-grained particles promote waterlogging. In the lowest topographic relief of the floodplain, if waterlogging is permanent, this prevent pedogenesis and soil development (e.g., Wright et al., 2000; Therrien et al., 2009; Varela et al., 2021).

5.1.3. Upper section of the Chorrillo Formation

This section is dominated by thick fine-grained floodplain deposits and thin dark fine-grained swamp/pond deposits. Paleosols are dominated by the Argentino Lake pedotype and in a minor proportion by the Chorrillo Malo Farm pedotype (argillic Vertisols) (Fig. 8).

This section records the stacking of hydromorphic Vertisols developed over distal floodplain deposits, and pedogenically unmodified crevasse splay deposits with sharp boundaries. Eventually, this pedotype is followed by swamp/pond deposits without pedogenesis. Towards the uppermost part of this section, argillic Vertisols developed over distal floodplain deposits (silty–muddy Fm facies) are interbedded with distal floodplain deposits without pedogenic modification.

As mentioned before, the Argentino Lake pedotype is a moderately-developed paleosol formed under conditions of seasonality of rainfall and/or waterlogged during a part of the year (seasonal waterlogging), and the Chorrillo Malo Farm pedotype is also moderately developed, but formed under better-drained conditions than the former pedotype. It is possible that the slightly coarser parent material (silt–mud) of this pedotype allowed the improvement of the drainage conditions in the floodplain. Similarly to the lower section of the unit, the interbedded of Vertisols - floodplain deposits without pedogenesis, the stacking of different profiles of the same Vertisol - swamp/pond deposits - floodplain deposits lacking pedogenic features, and the interbedded of argillic Vertisols - floodplain deposits without soil formation could represent the result of avulsion events in which the position of the channel changes within the floodplain. Also, the occurrence of different soil types (hydromorphic Vertisols *vs.* argillic Vertisols) in the floodplain could be the response to slightly different aggradation rates throughout this part of the floodplain which can result in subtle changes in topography affecting the local drainage. In addition, the relationship of Vertisols - swamp/pond deposits without pedogenesis suggests bad drainage conditions and fully permanent waterlogging in distal floodplain (e.g., Yeste et al., 2020; Varela et al., 2021).

The palynolgical analysis of the upper section add new information about this section of the Chorrillo Formation. As in the lower and middle sections, the most conspicuous plant element in swamps/ponds were water ferns of the Salviniales (Scafati et al., 2009). *Chomotriletes* is a freshwater alga that lives in subtropical shallow-water bodies (Davis, 1992), and probably had the same ecological requirements in the described assemblage. Additionally, some authors postulate that the presence of this algae indicates warm climatic areas with summer drought periods (local seasonal drying) (Scott, 1992; Carrión and Navarro 2002). Bryophytes and lycopsids of the upper section inhabited moist places, as along river banks and around swamp/ponds, probably associated with Liliales (see Fig. 8).

5.2. The significance of the paleosols of the Chorrillo Formation in the paleoenvironmental and paleoclimatic reconstruction

5.2.1. Paleoenvironment

Although five pedotypes have been differentiated through the Chorrillo Formation, they have in common the occurrence of redoximorphic features. These types of features are formed by processes of reduction, translocation and oxidation of Fe- and Mn-oxides in soils that are periodically saturated (Vepraskas, 1994, 2015). Such processes in a soil are known as aquic conditions, and typically floodplains can experience a combination of two forms of aquic conditions (Vepraskas, 1994, 2015). The first can be due to seasonal or periodic water saturation of the lower portion of the soil by ground water (i.e., ground water-gleying or endosaturation) (e.g., Kraus and Aslan, 1993; Vepraskas, 1994, 2015). The second, can be due to saturation of the upper portion of the soil by prolonged or seasonal perching of superficial water above an impermeable unit (i.e., surface-gleying, pseudogley or episaturation) (e.g., Kraus and Aslan, 1993; Vepraskas, 1994, 2015; PiPujol and Buuman, 1998).

Paleosols of the Chorrillo Formation appear to have resulted from a combination of both types of saturation or gleying. In this sense, it is possible to infer that aquic conditions by episaturation or surface-gleying took place in moderately-developed hydromorphic Vertisols and calcic Vertisols. Both pedotypes present redox depletion macro- and microfeatures associated to voids (fractures, root holes, bioturbation voids) of the surficial horizon (A), suggesting conditions of water stagnation developed on macropores without saturation of the entire matrix of the soil (e.g., Roquero et al., 2013; Vepraskas, 2015; Driese et al., 2016; Basilici et al., 2022). Although proximity to sand bodies (i.e., channel or crevasse splay deposits) could produce apparent pseudogley features because groundwater is easily transmitted through the most permeable beds to soil horizons, the clear association of the features of the A horizon to specific channels indicates a true pseudogley influence (Pipujol and Buurman, 1994; Licht et al., 2013). Episaturation probably was due to the impermeability of the unit that could be result from the high-density and low hydraulic conductivity of the fine-grained size parent materials (i.e., great content of clay in the groundmass) (e.g., Licht et al., 2013; Vepraskas, 2015; Basilici et al., 2022). Under this situation, water can remain stagnant on the surface and in the upper part of the soil for several days or weeks after major rainfalls or floods (Kraus and Aslan, 1993; Kraus and Hasiotis, 2006; Buol et al., 2011; Basilici et al., 2022). Also, these pedotypes present redox depletion features in root holes in the subsuperficial (B) horizon indicating that reducing conditions associated to macropores reach the lower horizon, probably associated to relatively shallow watertables (endosaturation or groundwater-gleying in B horizons).

Poorly-developed hydromorphic Vertisols and argillic Vertisols exhibit truncated profiles (without superficial horizon) that preclude them from determining conditions of the superficial horizon. However, the B horizon of the hydromorphic Vertisols shows evidence that the matrix was entirely saturated, probably due to ground water-gleying or endosaturation by a shallow watertable. In this regard, horizontal rhizoliths in Bssg horizons are evidence of anchorage of plants in a partially waterlogged setting where the watertable is high. Under high watertable conditions, roots develop an eco-physiologic adaptation looking for anchorage and as a response to the lack of aeration (e.g., Kraus and Hasiotis, 2006; Buatois and Mangano, 2011; Ashley et al., 2013; Brea et al., 2017; Raigemborn et al., 2018b). Meanwhile, the B horizon of argillic Vertisols present redox depletion features in root holes as those of the moderately developed hydromorphic Vertisols and calcic Vertisols, probably associated to endosaturation or groundwater-gleying.

On the other side, the entire profile (i.e., O, AB and B horizons) of the Histosols presents a gley matrix with redox concentrations occur around macropores (rhizoliths and voids) and also occur without relationship to macropores. The combination of redoximorphic features indicates that the matrix was wet for periods long enough for reducing conditions, while macropores become aerated. Vepraskas (2015) mentioned that this combined situation can take place if plants grow in the saturated horizon and transport air to their roots, as could be the case of the Chorrillo Formation due to the fact that there are evidences of plants that inhabited the swamp/ponds and their marginal settings (e.g., Vera et al., 2022; Perez Loinaze et al., 2023). However, redox concentration features in the matrix can respond to air trapped within the matrix. Such features can be found with episaturation and endosaturation (e.g., Vepraskas, 2014, 2015).

Even though it is not easily defined which of both factors (rainfall *vs.* floods) controlled stagnant water in the Chorrillo Formation pedotypes, the occurrence of non-pedogenized deposits intermingled with pedogenized ones (Fig. 2) attest to flood waters (flooding) because river floods led to an increase in the frequency of depositional events (e.g., Kraus, 1999; Wright et al., 2000; Flaig et al., 2013; Basilici et al., 2022). Soils that are often flooded, as those of the Chorrillo Formation, have relatively shallow watertables with strong seasonal variations leading to groundwater-gleying (Kraus and Aslan, 1993).

5.2.2. Paleoclimate

Several aspects of the paleosols macro- and micromorphology, clay mineral composition, pedogenic processes, and vegetation record give insight into the climatic conditions that prevailed in Southern Patagonia during the Maastrichtian Chorrillo Formation. Between these, the combination of redoximorphic (discussed above) and vertic features are indicative of seasonality of climate during soil formation (e.g., Basilici et al., 2022). In low-gradient fluvial system as those of the Chorrillo Formation, seasonality can be linked to (1) rainfalls, (2) watertable fluctuations, and (3) variations in fluvial discharge (e.g., Retallack, 2001; Therrien, 2005; Yeste et al., 2020; Varela et al., 2021). The intensity of rainfalls will condition watertables and the development of swamp/ponds settings in the floodplain (e.g., Varela et al., 2021), as success in the Chorrillo Formation. Kraus and Aslan (1993) point out that avulsion, a typical mechanism of the studied unit, can be induced by unusual large flood during wetter periods because change in precipitations can influence avulsion frequency. If this could be the case of the Chorrillo Formation, each avulsion event throughout the unit could respond to a period of wetter conditions.

Modern Vertisols, typically occur in environments with mean annual precipitations between 500 and 1000 mm, but may occur in much better climate as well if extremely high precipitations are compensated by high temperatures and evapotranspiration (Kovda, 2020). Vertic features throughout the entire section of the Chorrillo Formation attest to formation under seasonal rainfalls, which control wet and dry cycles causing alternating wetting and drying of the soil and the swelling and shrinking of expandable clays (e.g.,Varela et al., 2018; Basilici et al., 2022). In Vertisols, the main pedotype recorded at Chorrillo Formation, smectite originated through inheritance (detrital) or pedogenic (*in situ*) (Wilson, 1999). Although we did not utilize SEM analysis allowing to confirm the origin of the smectite (e.g., Raigemborn et al., 2014; Song et al., 2018), the overall combination of well and poorly crystallized smectites in Chorillo paleosols could suggest the occurrence of both detrital and pedogenic smectites (e.g., Chamley, 1989; Srivastava et al., 2002; Raigemborn et al., 2014). However, the high quantity of smectite in C horizons (i.e., floodplain deposits without pedogensis) is evidence of the detrital origin of this clay mineral component in the parent material of the paleosols (e.g., Basilici et al., 2022). Illite is the second clay mineral in order of abundance of the Chorrillo paleosols (<30%; average of 10% through the entire section). Illite is another clay mineral reported as abundant in Vertisols (Coulombe et al., 1996), and it is commonly inherited from parent rocks and do not typically form during pedogenesis (Chamley, 1989; Wilson, 1999). Minor contents of chlorite (0–20%, 3% on average), kaolinite (0–15%, 2% on average) and mixed layers of illite-smectite (0–10%, 2% on average) through the unit can also be consider detrital in origin (Wilson, 1999; Raigemborn et al., 2014).

Another paleoclimate proxy is the occurrence of pedogenic carbonates. Although they may form under a wide range of temperatures and rainfalls (e.g., Sheldon and Tabor, 2009; Raigemborn et al., 2018b, 108c), the limit to calcite formation is the episodic drying of the soil for a long period (e.g., Kraus and Hasiotis, 2006). In this case study, the characteristics of pedogenic carbonate nodules of the calcic Vertisols (i.e., the relatively large size [> 20 mm in diameter], micritic in composition, presence of sparitic veins), the intergrowth of iron oxides and carbonate, and their occurrence in horizons with vertic features (Bssk horizons), indicate formation under seasonal climates, in which precipitation is spread over a limited period of three to four months (e.g., Khadkikar et al., 2000; Therrien et al., 2009). Such features (together with the dominance of smectite in the groundmass and in the calcite nodules, and the presence of scarce–moderate [<15%] proportions of kaolinite, mainly in the nodules), attest for a relatively warm and humid (1000–1200 mm/year) climate, with seasonal rainfall (e.g., Raigemborn et al., 2018b, 2018c).

Although rhizoliths and rhizohaloes are the only macro-record of vegetal cover, the overall palynoflora recovered along the entire section of the Chorrillo Formation contains elements with ecological requirements that agree with the result of paleosols analysis. Among them, representatives of aquic ferns (Salviniaceae and Marsiliaceae), Arecaceae and Araceae (Perez Loinaze et al., 2023) are interpreted as markers of tropical or subtropical climates (Kramer and Green, 1990; Friis et al., 2004; Bakker et al., 2011). Conversely, some elements as Podocarpaceae (in particular *Phyllocladidites mawsonii*) and Proteaceae are related to temperate climates (Baldoni and Askin, 1993; Vajda and Bercovici, 2012). Given these results, a mixed flora is recognized, pointing to temperate to warm conditions. On the other hand, the abundance and richness of terrestrial ferns, and other spore producing taxa (e.g., bryophytes, lycopsids), along with the conifer family Podocarpaceae through the Chorrillo Formation, can be interpreted as indicators of relatively humid conditions (Hill and Brodribb, 1999; Schrank, 2010). Additionally, there is paleobotanical evidence of rainfall seasonality. For example, well-developed growth rings in the fossil woods of the lower section of the unit (see Fig. 2) suggests periods of arrested growth (seasonality) (Novas et al., 2019). Also, the existence of the algae Zygnemataceae in hydromorphic Vertisols and Histosols and in the megafloristic level 1 in the middle section of the unit (see Fig. 2), indicate warm conditions, at least during a part of the year, and seasonality of rainfall, which is necessary to stimulate the formation of zigospores (Jarzen, 1979). The record of *Classopollis* in a calcic Vertisol-like paleosol, and in samples associated with swamp/pond deposits without pedogenesis and with the level bearing phytodetritus of the lower section of the unit, and in the Argentino Lake pedotype linked to the *Magallanodon* Site of the middle section (see Fig. 2), also indicate seasonal rainfall (Abbink, 1998; Sajjadi and Playford, 2002). Similarly, the record of abundant cysts of the algae *Chomotriletes minor*, in a Vertisol-like paleosol of the uppermost part of the unit (see Fig. 2) could possibly be an indicator for relatively warm climates with local seasonal drying (Scott, 1992). However, the presence of organic horizons (O) formed from carbonized plant debris within the Centinela River pedotype dismiss the existence of a dry-season during their formation, because under dry conditions organic matter is oxidized preventing the accumulation of peats (e.g., Wright et al., 2000). Such horizons are found in very wet settings (e.g., wetlands) where watertable is very high and plant debris decomposes less rapidly due to low oxygen conditions (e.g., Vepraskas and Croft, 2016).

Variation in drainage conditions detected throughout the paleosols developed within the floodplain of the Chorrillo Formation could be a response to climate change (low-frequency scale allogenic factor), and such climate changes must be associated to sharp sedimentological changes through the unit. Although very subtle sedimentological changes over the entire succession allowed us to define informally three sections (lower, middle and upper), no big changes in the fluvial style were recognized. This could be due to the constant dominance of fine-grained deposits and to the lack of significant erosion surface recorded in the studied area (e.g., Moyano-Paz et al., 2022a). Also, Moyano-Paz et al. (2022a) explain that the alternation of channelized complex sandy narrow sheet and complex gravelly narrow sheet elements was probably related to small fluctuations in the sedimentary supply/accommodation space ratio. Also, similarities in clay mineralogy in all the paleosols (mainly smectite) suggest uniformity in climate conditions during their formation. Consequently, variations in drainage conditions of paleosol types of the Chorrillo Formation can be linked to the topographic location within the fluvial floodplain, and the grain-size (parent material) of the parent material, which in turn are associated to avulsion events, and do not reflect the control of allogenic factors such as the climate.

The studied succession lies over the fluvial La Irene Formation of a latest Campanian-Maastrichtian age (Ghiglione et al., 2021), and below the marine Calafate Formation which is assigned to the latest Maastrichtian in the study area (Marenssi et al., 2004; Ghiglione et al., 2021) but that may reach a Danian age toward the south (Davis et al., 2022). Thus, the Chorrillo Formation provides insight into the climate conditions during the Maastrichtian, an age recently confirmed by the palynostratigraphic analysis made by Perez Loinaze et al. (2023). The Maastrichtian was described as a global long-term climatic cooling trend following peak warmth during the mid-Cretaceous, during which pulses of warming were detected (e.g., Li et al., 2018). However, there is distinct climatic distribution pattern in various latitudinal zones (Scotese, 2005). Although up to now not quantitatively estimate paleoclimatic conditions (i.e., from the use of climofunctions) of the Maastrichtian Chorrillo Formation were performed, our interpretations based on paleosols correspond with previous results reported from a palynological study (Perez Loinaze et al., 2023) indicating an overall temperate or warm-temperate and seasonally humid climate. Such climate prevailed in the mid–high paleolatitudes (~ 54° paleo-S following van Hinsbergen et al., 2015) in the Austral-Magallanes Basin during the Maastrichtian. Climate conditions interpreted in our study are also supported by the global distribution of reconstructed paleoclimates based on the climate indicative and climate sensitive deposits of Scotese (2005) and Boucout et al. (2013), who mentioned the existence of a Warm-Temperate Zone for mid-paleolatitudes (30−60° N and S) during the Maastrichtian. We consider that future studies based on geochemical and isotopic paleoclimate indices of the Chorrillo Formation paleosols, could help to improve our understanding about Maastrichtian climates at mid−high paleolatitudes of the Southern Hemisphere.

6. Conclusions

We interpreted that the dinosaur-bearing Chorrillo Formation (Maastrichtian; ~500 m thick) in the Austral-Magallanes Basin (south Patagonia, Argentina) contain paleosols which are smectite-rich moderately-developed hydromorphic Vertisol-, calcic Vertisol-, poorly-developed hydromorphic Vertisol-, Histosol-, and argillic Vertisol-like paleosols (Argentino Lake, Perito Moreno Glacier, Anita Farm, Centinela River and Chorrillo Malo Farm pedotypes, respectively). Such paleosols constitute more than the 60% of the entire thickness of the studied succession. They were developed in different settings of the distal floodplain of a low gradient fluvial system in which mainly vertic and hydromorphic processes with variations in drainage conditions took place. Redoximorphic features of these paleosols indicate that they have resulted from a combination of surface-gleying (episaturation) and ground water-gleying (endosaturation), which respond to relatively shallow watertables with strong seasonal variations, probably controlled by flood waters (flooding). The small-scale or high frequency stacking of the Chorrillo Formation paleosols indicate that, although without significant changes in facies association of the floodplain, variations in drainage conditions of the soils are linked to slightly topographic location within the distal floodplain, subtle grain-size differences of the parent material, and variations in flooding duration. The vertical stacking of these paleosols throughout the unit results from the avulsions and “cryptic” avulsions of the channel. The distribution of the paleobotanical remains within the unit show different ecological preferences for the inhabited place. This study demonstrates that even where exposures are of poor quality and prevent a detailed lateral analysis in cross-sections, paleosols-floodplain relations can be explained throughout a low gradient fluvial system section.

Paleosols of the studied unit produce abiotic climate proxy suggesting overall temperate/temperate–warm and seasonally humid conditions for their formation time, which agree with biotic climate proxy coming from the paleobotanical record of the unit. These new reconstructions provide insight into the terrestrial paleoenvironmental and paleoclimatic conditions in the mid−high paleolatitudes of southern Argentinean Patagonia during the Maastrichtian. Although our interpreted climate conditions agree with global distribution of reconstructed cretaceous climates, future geochemical and isotopic paleoclimate indices of the Chorrillo Formation paleosols, could help to improve our understanding about Maastrichtian climates of the Southern Hemisphere.

Acknowledgments

The present paper is the result of a joint Argentine-Japanese exploration, carried out in March 2020 and March 2022. Dr. Yoshihiro Hayashi, former Director General, National Museum of Nature & Science, Japan, for his support for the project by funding a major part of the expedition from the internal grant from the museum. Financial and logistical support for these studies was provided by the projects PIP 100523 of the CONICET and the PI+D N890 of the UNLP (to MSR). The authors would like to thank Oscar Canto and Carla Almazán (Secretaría de Cultura) for supporting our projects and explorations in Santa Cruz,

F. Echeverría, D. Fraser and A. Prieto for the hospitality and their valuable geographic knowledge of the Anita territories. Authors would also like to thank the entire crew, including C. Sakata, C. Miyamae, H. Kamei, T. Tsuihiji, F. Brissón-Egli, A. Moreno, G. Lio, S. Miner, G. Muñoz, J. De Pasqua, C. Thompson, D. Piazza, G. Lo Coco, A. Misantone, G. Stoll, F. Agnolín, S. Rozadilla, A.M. Aranciaga Rolando, M.J. Motta, and M.P Isasi for the spectacular assistance and logistics during fieldwork. The authors are very grateful to two reviewers (William Lukens and Giorgio Basilici) and to the editor of the journal (Eduardo Koutsoukos) for highly constructive reviews.

References

Abbink, O.A., 1998. Palynological investigation in the Jurassic of the North Sea region. Laboratory of Palaeobotany and Palynology, Contributions Series, LPP Foundation Utrecht 8; 192 p.

Adamson, K., Candy, I., Whit, L., 2015. Coupled micromorphological and stable isotope analysis of Quaternary calcrete development. Quat. Res. 84, 272–286.

Ahmad, N., 1983. Vertisols. In: Wilding, N.L.P., Smeck, E., Hall, G.F. (Eds.), Pedogenesis and Soil Taxonomy II. The Soil Orders. Developments in Soil Science, 11B. Elsevier, Amsterdam, pp. 91-123.

Ahmad, N., Mermut, A., 1996. Vertisols and technologies for their management. In: Ahmad, N., Mermut, A. (Eds.), 1996. Developments in Soil Science, 24. Elsevier, Amsterdam, p. 549.

Alonso-Zarza, A.M., Sanz, M.E., Calvo, J.P., Estcvez, P., 1998. Calcified root cells in Miocene pedogenic carbonates of the Madrid Basin: evidence for the origin of Microcodium b. Sediment. Geol. 16, 81–97.

Aranciaga Rolando, A.M., Motta, M.J., Agnolín, F.L., Manabe, M., Tsuihiji, T., Novas, F.E. 2022. A large Megaraptoridae (Theropoda: Coelurosauria) from Upper Cretaceous (Maastrichtian) of Patagonia, Argentina. Scientific Reports 12, 6318.

Ashley, G., Deocampo, D.M., Kahmann-Robinson, J.A., Driese, S., 2013. Groundwater-fed wetland sediments and paleosols: it's all about water table. In: Driese, S.G., Nordt, L.C. (Eds.), New Frontiers in Paleopedology and Terrestrial Paleoclimatology: Paleosols and

Soil Surface Analogue Systems. Society for Sedimentary Geology, Special Publication. 104. pp. 47–61.

Baldoni, A.M., Askin, R.A., 1993. Palynology of the Lower Lefipán Formation (Upper Cretaceous) of Barranca de Los Perros, Chubut Province, Argentina. Part II. Angiosperm pollen and discussion. Palynology 17, 241–264.

Baker, W.J., Norup, M.V., Clarkson, J.J., Couvreur, T.L., Dowe, J.L., Lewis, C.E., Pintaud, J.C., Savolainen, V., Wilmot, T., Chase, M.W., 2011. Phylogenetic relationships among arecoid palms (Arecaceae: Arecoideae). Annals of Botany 108, 1417–32.

Basilici, G., Colombera, L., Soares, M.V.T., Arévalo, O.J., Mountney, N.P., Lorenzoni, P., de Souza Filho C.R., Ferreira Mesquita, A., JanockoJ., 2022 Variations from dry to aquic conditions in Vertisols (Esplugafreda Formation, Eastern Pyrenees, Spain): Implications for late Paleocene climate change. Palaeogeography, Palaeoclimatology, Palaeoecology 595, 110972. https://doi.org/10.1016/j.palaeo.2022.110972.

Batten, D.J., 1975. Wealden palaeoecology from the distribution of plant fossils. Proceedings of the Geologists Association 85, 433–458.

Beilinson, E., Raigemborn, M.S., 2013. High-frequency controls on alluvial successions: an integrated sedimentological and palaeopedological approach to the Plio- Pleistocene of Argentina. Quat. Int. 317, 34–52.

Biddle, K., Uliana, M., Mitchum Jr., R., Fitzgerald, M., Wright, R. 1986. The stratigraphic and structural evolution of central and eastern Magallanes Basin, Southern America. In: Allen, P., Homewoods, P., (Eds.), Foreland Basins, vol 8. International Association of Sedimentologists Special Publication pp. 41-61.

Birkeland, P.W., 1999. Soils and Geomorphology. Oxford University Press, New York (430 pp).

Biscaye, P.E., 1965. Mineralogy and Sedimentation of Recent Deep-Sea Clay in the Atlantic Ocean and Adjacent Seas and Oceans, vol. 76. Geological Society of America Bulletin, pp. 803–832.

Bonaparte, J.F. 1996. Dinosaurios de América del Sur, 2da Edición. Museo Argentino de Ciencias Naturales “Bernardino Rivadavia”, Buenos Aires, Argentina, p. 174.

Boucot, A.J., Xu, C., Scotese, C.R., Morley, R.J., 2013. Phanerozoic paleoclimate: an atlas of lithologic indicators of climate. SEPM Concepts in Sedimentology andPaleontology 11. https://doi.org/10.2110/sepmcsp.11.

Brea, M., Zucol, A.F., Bargo, M.S., Fernicola, J.C., Vizcaíno, S.F., 2017. First Miocene record of Akaniaceae in Patagonia (Argentina): a fossil wood from the early Miocene Santa Cruz Formation and its palaeobiogeographical implications. Bot. J. Linn. Soc. 183, 334–347.

Brown, G., Brindley, G.W., 1980. X-ray diffraction procedures for clay mineral identification. In: Brindley, G.W., Brown, G. (Eds.), Crystal Structures of Clay Minerals and their X-Ray Identification. Mineralogical Society, London, pp. 305–359.

Bullock, P., Fedoroff, N., Jongerius, A., Stoops, G., Tursina, T., 1985. Handbook for Soil Thin Section Description. Waine Research Publications, p. 152.

Buol, W.S., Southard, R.J., Graham, R.C., McDanield, P.A., 2011. Soil Genesis and Classifications, sixth ed. Wiley-Blackwell, Oxford, p. 543.

Buatois, L.A., Mangano, M.G., 2011. Ichnology: Organism-Substrate Interations in Space and Time. Cambridge University Press, Cambridge (358 pp).

Carrión, J.S., Navarro, C., 2002. Cryptogam spores and other non-pollen microfossils as sources of palaeoecological information: case-studies from Spain. Annals Botanical Fennici 39, 1–14.

Chamley, H., 1989. Clay Sedimentology. Springer-Verlag, Berlin, 623 pp.

Chimento, N.R., Agnolín, F.L., Tsuihiji, T., Manabe, M., Novas, F.E., 2020. New record of a Mesozoic gondwanatherian mammaliaform from Southern Patagonia. Science and Nature 107 (6), 1–7.

Chimento, N.R., Agnolín, F.L., Novas, F.E., Manabe, M., Tsihuiji, M., 2021. New gondwanatherian (Mammaliaformes) remains from the Chorrillo Formation (Late Cretaceous) of Southern Patagonia, Argentina. Cretaceous Research 127, 104947.

Coulombe, C.E., Wilding, L.P., Dixon, J.B., 1996. Overview of Vertisols: characteristics and impacts on society. In: Advances in Agronomy, 57. Elsevier, pp. 289-375.

Cuitiño, J.I., Varela, A.N., Ghiglione, M.C., Richiano, S., Poiré, D.G. 2019. The Austral-Magallanes Basin (southern Patagonia): A Synthesis of its stratigraphy and evolution. Latin American Journal of Sedimentology and Basin Analysis 26 (2), 155-166.

Davis, O.K., 1992. Rapid climatic change in coastal southern California inferred from Pollen Analysis of San Joaquin Marsh. Quaternary Research 37, 89–100.

Dobbs, S.C., Malkowski, M.A., Schwartz, T., Sickmann, Z.T., Graham, S.A. 2022. Depositional controls on detrital zircon provenance: An example from Upper Cretaceous strata, southern Patagonia. Frontiers in Earth Science 10, 824930.

Driese, S.G., Peppe, D.J., Beverly, E.J., Di Pietro, L.M., Arellano, L.N., Lehmann, T., 2016. Paleosols and paleoenvironments of the early Miocene deposits near Karungu, Lake Victoria, Kenya. Palaeogeogr. Palaeoclimatol. Palaeoecol. 443, 167–182. https://doi.org/10.1016/j.palaeo.2015.11.030.

Feruglio, E., 1945. Estudios geológicos y glaciológicos en la región del Lago Argentino (Patagonia). Boletín de la Academia Nacional de Ciencias de Córdoba 37 (1), 3-255.

Filatoff, J., 1975. Jurassic palynology of the Perth basin, Western Australia. Palaeontographica, Abteilung B 154, 1–113.

Flaig, P.P., McCarthy, P.J., Fiorillo, A.R., 2013. Anatomy, evolution and paleoenvironmental interpretation of an ancient arctic coastal plain: integrated paleopedology and palynology from the Upper Cretaceous (Maastrichtian) Prince Creek Formation, North Slope, Alaska. In: In: Driese, S.G., Nordt, L.C. (Eds.), New Frontiers in Paleopedology and Terrestrial Paleoclimatology: Paleosols and Soil Surface Analogue Systems, vol. 104. Society for Sedimentary Geology, Special Publication, pp. 179–230.

Friis, E.M., Pedersen, K.R., Crane, P.R., 2004. Araceae from the Early Cretaceous of Portugal: Evidence on the emergence of monocotyledons. PNAS 101, 16565–16570.

Ghiglione, M.C., Rocha, E., Raggio, M.F., Ramos, M.E., Ronda, G., Moyano-Paz, D., Varela, A.N., Valencia, V. 2021. Santonian-Campanian continentalization in the Austral-Magallanes basin: Regional correlation, provenance and geodynamic setting. Cretaceous Research 128, 104968.

Gibling, M.R., 2006. Width and thickness of fluvial channel bodies and valley fills in the geological record: a literature compilation and classification. J. Sediment. Res. 76, 731–770.

Gile, L.H., Peterson, F.F., Grossman, J.B., 1966. Morphological and genetic sequences of carbonate accumulation in desert soils. Soil Sci. 101, 347–360.

Hill, R.S., Brodribb, T.J., 1999. Turner Review No. 2. Southern Conifers in Time and Space. Australian Journal of Botany 47, 639–696.

Imbellone, P.A., Guichon, B.A., Gim´enez, J.E., 2009. Hydromorphic soils of the Río de la Plata coastal plain, Argentina. Lat. Am. J. Sedimentol. Basin Anal. 16, 3–18

Jarzen, D., 1979. Zygospores of zygnemataceae in the Paleocene of southern Saskatchewan (Canada). Review of Palaeobotany and Palynology 28, 21–25.

Kahmann, J.A. Seaman III, J., Driese, S.G., 2008. Evaluating Trace Elements as Paleoclimate Indicators: Multivariate Statistical Analysis of Late Mississippian Pennington Formation Paleosols, Kentucky, U.S.A. J. Geol. 116, 254-268.

Kahmann, J.A., Driese, S.G., 2008. Paleopedology and geochemistry of Late Mississippian (Chesterian) Pennington Formation paleosols at Pound Gap, Kentucky, USA: Implications for high-frequency climate variations. Palaeogeography, Palaeoclimatology, Palaeoecology 259, 357-381.

Khadkikar, A.S., Chamyal, L.S., Ramesh, R., 2000. The character and genesis of calcrete in Late Quaternary alluvial deposits, Gujurat, western India, and its bearing on the interpretation of ancient climates. Palaeogeography, Palaeoclimatology, Palaeoecology 162, 239–261.

Kovda, I., 2020. Vertisols: extreme features and extreme environment. Geoderma Reg. 22, e00312.

Kovda, I., Mermut, A., 2010. Vertic features. In: Stoops, G., Marcelino, V., Mees, F. (Eds.), Interpretation of Micromorphological Features of Soils and Regoliths. Elsevier, Amsterdam, pp. 109–127.

Kovda, I., Mermut, A., 2018. Vertic features. In: Stoops, G., Marcelino, V., Mees, F. (Eds.), Interpretation of Micromorphological Features of Soils and Regoliths (Second Edition). Elsevier, pp. 605-632.

Kramer K., Green, P.S., 1990. Pteridophytes and Gymnosperms. In: Kubitzki K. (Ed.) The families and genera of vascular plants, Volumen I, Springer–Verlag, Berlin.

Kraus, M.J., 1996. Avulsion deposits in lower Eocene alluvial rocks, Bighorn Basin, Wyoming. Journal of Sedimentary Research 66, 354-363

Kraus, M.J., 1999. Paleosols in clastic sedimentary rocks. Earth Sci. Rev. 47, 41–70.

Kraus, M.J., 1997. Lower Eocene alluvial paleosols: pedogenic development, stratigraphic relationships, and paleosol/landscape associations. Palaeogeography, Palaeoclimatology, Palaeoecology 129, 387–406.

Kraus, M.J., Aslan, A., 1993. Eocene hydromorphic paleosols: significance for interpreting ancient floodplain processes. J. Sediment. Petrol. 63, 453–463.

Kraus, M.J., Bown, T.M., 1993. Short-term sediment accumulation rates determined from Eocene alluvial paleosols. Geology 21, 743–746.

Kraus, M.J., Hasiotis, S.T., 2006. Significance of different modes of rhizolith preservation to interpreting paleoenvironmental and paleohydrologic settings: examples from Paleogene paleosols, Bighorn Basin, Wyoming, U.S.A. J. Sediment. Res. 76, 633–646.

Li, J., Wen, X., Huang, C., 2020. Lower and upper Cretaceous paleosols in the western Sichuan Basin, China: Implications for regional paleoclimate. Geological Journal, 55, 390-408.

Licht, A., Cojan, I. Caner, L., Soe, A.N., Jaeger, J.J., France-Lanord, C., 2014. Role of permeability barriers in alluvial hydromorphic palaeosols: The Eocene Pondaung Formation, Myanmar. Sedimentology 61, 362-382.

Lindbo, D.L., Stolt, M.H., Vepraskas, M.J., 2010. Redoximorphic Features. In: Stoops, G., Marcelino, V., Mees, F. (Eds.), Interpretation of Micromorphological Features of Soils and Regoliths. Elsevier, Amsterdam, pp. 129–147.

Lizzoli, S., Raigemborn, M.S., Varela, A.N. 2021. Controls of pedogénesis in a fluvial-eolian succession of Cenomanian age in northern Patagonia. Palaeogeography, Palaeoclimatology, Palaeoecology 577, 110549.

Macellari, C.E., Barrio, C.A., Manassero, M.J. 1989. Upper Cretaceous to Paleocene depositional sequences and sandstone petrography of southwestern Patagonia (Argentina and Chile). Journal of South American Earth Sciences 2, 223-239.

Machette, M.N., 1985. Calcic soils of the southwestern United States. Geol. Soc. Am. Spec. Pap. 203, 1–21. http://dx.doi.org/10.1130/SPE203-p1.

Mack, G.H., James, W.C., Monger, H.C., 1993. Classification of paleosols. Geol. Soc. Am. Bull. 105, 129–136.

Malkowski, M.A., Sharmann, G.R., Graham, S.A., Fildani, A. 2017. Characterisation and diachronous initiation of coarse clastic deposition in the Magallanes-Austral foreland basin. Basin Research 29, 298-326.

Manríquez, L.M.E., Lavina, E.L.C. Fernández, R.A., Trevisan, C., Leppe, M.A. 2019. Campanian-Maastrichtian and Eocene stratigraphic architecture, facies análisis, and paleoenvironmental evolution of the northern Magallanes Basin (Chilean Patagonia). Journal of South American Earth Sciences 93, 102-118.

Marriott, S.B., Wright, V.P., 1993. Palaeosols as indicators of geomorphic stability in two Old Red Sandstone alluvial suites, South Wales. J. Geol. Soc. Lond. 150, 1109–1120.

Mermut, A.R., Dasog, G.S., Dowuona, G.N., 1996. Soil morphology. In: Ahmad, N., Mermut, A. (Eds.), Vertisols and Technologies for their Management. Developments in Soil Science, vol. 24. Elsevier, Amsterdam, pp. 43-61.

Moore, D.M., Reynolds Jr., R.C., 1997. X-Ray Diffraction and the Identification and Analysis of Clay Minerals. Oxford University Press, Oxford.

Moyano-Paz, D., Richiano, S., Varela, A.N., Gómez-Dacal, A.R., Poiré, D.G., 2020. Ichnological signatures from wave- and fluvial-dominated deltas: the La Anita Formation, Upper Cretaceous, Austral-Magallanes Basin. Patagonia: Marine and Petroleum Geology 114, 104168.

Moyano-Paz, D., Rozadilla, S., Agnolin, F., Vera, E., Coronel, M.D., Varela, A.N., Gómez-Dacal, A.R., Aranciaga-Rolando, A.M., D’Angelo, J.S., Pérez-Loinaze, V., Richiano, S., Chimento, N.R., Motta, M.J., Sterli, J., Manabe, M., Takanobu, T.,Isasi, M.P., Poiré, D.G., Novas, F.E. 2022a. The uppermost Cretaceous continental deposits (UCCD) at southern end of Patagonia, the Chorrillo formation case study (Austral-Magallanes Basin): Sedimentology, fossil content and regional implications. Cretaceous Research 130, 105059.

Moyano-Paz, D., Gómez-Dacal, A.R., Varela, A.N., Comerio, M., Muñoz-Olivero, T.M., Bucher, J., Richiano, S., Poiré, D.G. 2022b. Control son composition and diagénesis of wave- and river-dominated deltas: impacts on reservoir properties. An Example from the La Anita Formation (Argentina). Marine and Petroleum Geology 138, 105571.

Moyano-Paz, D., Isla, M.F., MacEachern, J.A., Richiano, S., Gómez-Dacal, A.R., Varela, A.N., Poiré, D.G. 2022c. Evolution of an aggradational wave-dominated delta: Sediment balance and animal-substrate dynamics (Upper Cretaceous La Anita Formation, Southern Patagonia). Sedimentary Geology 437, 106193.

Munsell Color, 2013. Munsell Soil-Color Charts. Munsell Color, Grand Rapids, M.

Noetinger, S., Pujana, R.R., Burrieza, A., Burrieza, H.P., 2017. Use of UV-curable acrylates gels as mounting media for palynological samples. Revista del Museo Argentino de Ciencias Naturales Nueva Serie 19, 19–23.

Novas, F.E., Agnolin, F.L., Rozadilla, S., Aranciaga-Rolando, A.M., Brisson-Egli, F., Motta, M.J., Cerroni, M., Ezcurra, M.D., Martinelli, A.G., D´Angelo, J.S., Alvarez-Herrera, G., Gentil, A.R., Bogan, S., Chimento, N.R., García-Marsà, J.A., Lo Coco, G., Miquel, S.E., Brito, F.F., Vera, E.I., Perez Loinaze, V.S., Fernández, M.S., Salgado, L., 2019. Paleontological discoveries in the Chorrillo Formation (upper Campanian-lower Maastrichtian, Upper Cretaceous), Santa Cruz Province, Patagonia, Argentina. Revista del Museo Argentino de Ciencias Naturales, Nueva Serie, 21(2): 217–293.

Odino-Barreto, A.L., Cereceda, A., Gómez-Peral, L.E., Coronel, M.D., Tettamanti, C., Poiré, D.G., 2018. Sedimentology of the shallow marine deposits of the Calafate formation during the maastrichtian transgression at Lago Argentino, Austral-Magallanes Basin, Argentina. Latin American Journal of Sedimentology and Basin Analysis 25 (2), 169-191.

Pal, D.K., Wani, S.P., Sahrawat, K.L., 2012. Vertisols of tropical Indian environments: Pedology and edaphology. Geoderma 189-190, 28-49.Pankhurst, R.J., Riley, T.R., Fanning, C.M., Kelley, S.P. 2000. Episodic silicic volcanism in patagonia and Antartic Peninsula: Chronology of magmatism associated with the break-up of Gondwana. Journal of Petrology 41, 605–625.

Perez Loinaze, V.S., Vera, E.I., Moyano-Paz, D., Coronel, M.D., Manabe, M., Tsuihiji, T., Novas, F.E., 2023. Maastrichtian palynological assemblages from the Chorrillo Formation, Patagonia, Argentina. Review of Palaeobotany and Palynology, 104893 https://doi.org/10.1016/j.revpalbo.2023.104893

Phipps, D., Playford, G., 1984. Laboratory techniques for extraction of palynomorphs from sediments. Papers of the Department of Geology, University of Queensland vol. 11, 1–23.

PiPujol, M.D., Buurman, P., 1998. Analyzing ground-water gley and surface-water (pseudogley) effects in paleosols. Quat. Int. 51-52, 77–79.

Platt, N.H. and Keller, B. 1992. Distal alluvial deposits in a foreland basin setting -the Lower Freshwater Molasse (Lower Miocene), Switzerland: sedimentology, architecture and palaeosols. Sedimentology, 39, 545–565, https://doi.org/ 10.1111/j.1365-3091.1992.tb02136.x

Raigemborn, M.S., Gómez-Peral, L.E., Krause, J.M., Matheos, S.D., 2014. Controls on clay minerals assemblages in an early Palaeogene nonmarine succession: implications for the volcanic and paleoclimatic record of extra-andean patagonia, Argentina. Journal of South American Earth Sciences 52, 1–23

Raigemborn, M.S., Beilinson, E., Krause, J.M., Varela, A.N., Bellosi, E., Matheos, S., Sosa, N., 2018a. Paleolandscape reconstruction and interplay of controlling factors of an Eocene pedogenically-modified distal volcaniclastic succession in Patagonia. J. S. Am. Earth Sci. 86, 475–496.

Raigemborn, M.S., Krapovickas, V., Beilinson, E., Peral, L.E.G., Zucol, A.F., Zapata L. and Sial, A.N. 2018b. Multiproxy studies of Early Miocene pedogenic calcretes in the Santa Cruz Formation of southern Patagonia, Argentina indicate the existence of a temperate warm vegetation adapted to a fluctuating water table. Palaeogeography, Palaeoclimatology, Palaeoecology, 500, 1–23.

Raigemborn, M.S., Krapovickas, V. et al. 2018c. Paleosols and related soil-biota of the early Miocene Santa Cruz Formation (Austral-Magallanes Basin, Argentina): a multidisciplinary approach to reconstructing ancient terrestrial landscapes. Latin American Journal of Sedimentology and Basin Analysis, 25, 117–148

Raigemborn, M.S., Lizzoli, S., Hyland, E., Cotton, J., Gómez-Peral, L.E., Beilinson, E., Krause, M. 2022. A paleopedological approach to understanding Eocene environmental conditions in southern Patagonia, Argentina. Palaeogeography, Palaeoclimatology, Palaeoecology 601, 111129.

Retallack, G.J., 1988. Field recognition of paleosols. Geol. Soc. Am. Spec. Pap. 216, 1–20.

Retallack, G.J., 1991. Untangling the effects of burial alteration and ancient soil formation. Annual Review of Earth Planetary Sciences 19, 183–206.

Retallack, G.J., 1993. Classification of paleosols: discussion and reply. Discuss. Geol. Soc. Am. Bull. 105, 1635–1636.

Retallack, G.J., 1994. A pedotype approach to latest cretaceous and earliest Tertiary paleosols in eastern Montana. Geol. Soc. Am. Bull. 106, 1377–1397.

Retallack, G.J., 1998. Core concepts in paleopedology. Quaternary International 51/52, 203–212.

Retallack, G.J. 2001. Soils of the past: An introduction to Paleopedology, Second Edition. Blackwell Science, Oxford, 404 pp.

Roquero, E., Silva, P.G., Zazo, C., Goy, J.L., Dabrio, C.J., Borja, F., 2013. Micromorphology of hydromorphic soils developed in fluvio-marine sediments during the Middle-Late Pleistocene transit in the Gulf of Cadiz (Atlantic South Spain). Spanish J. Soil Sci. 3, 184–200.

Rozadilla, S., Agnolín, F.L., Manabe, M., Tsuihiji, T., Novas, F.E., 2021. Ornithischian remains from the Chorrillo Formation (Upper Cretaceous) of Southern Patagonia, Argentina, and their implications on Ornithischian paleogeography in the Southern Hemisphere. Cretaceous Research 125, 104881.

Sacristán-Horcajada, S., Arribas, M.E., Mas, R., 2016. Pedogenetic calcretes in early Synrift alluvial systems (Upper Jurassic, West Cameros Basin), northern Spain. J. Sediment. Res. 86, 268–286. http://dx.doi.org/10.2110/jsr.2016.30.

Sajjadi, F., Playford, G., 2002. Systematic and stratigraphic palynology of the Late Jurassic-earliest Cretaceous strata of the Eromanga Basin, Queesland, Australia. Palaeontographica Abt. B 261, 99–165.

Scafati, L., Melendi, D.L., Volkheimer, W., 2009. A Danian subtropical lacustrine paynobiota from South America (Bororó Formation, San Jorge Basin, Patagonia – Argentina). Geologica Acta 7, 35–61.

Schoeneberger, P.J., Wysocki, D.A., Benham, E.C., Soil Survey Staff, 2012. Field Book for Describing and Sampling Soils, Version 3.0. Natural Resources Conservation Service. National Soil Survey Center, Lincoln, NE, pp. 9–14.

Schrank, E., 2010. Pollen and spores from the Tendaguru Beds, Upper Jurassic and Lower Cretaceous of southeast Tanzania: palynostratigraphical and paleoecological implications. Palynology 34, 3–42.

Schultz, L.G., 1964. Quantitative interpretation of mineralogical composition from X-ray and chemical data for Pierra Shale. In: U.S. Geological Survey Professional, 391, pp. 1–31.

Scotese, C.R., 2005. Paleomap project. http://www.scotese.com.

Scott, L., 1992. Environmental Implications and Origin of Microscopic Pseudoschizaea Thiergart and Frantz Ex R. Potonie emend. Journal of Biogeography 19, 349–354.

Sheldon, N.D., 2003. Pedogenesis and geochemical alteration of the picture gorge subgroup, Columbia River Basalt, Oregon. Geological Society of America Bulletin 115, 1377–1387

Sheldon, N.D., Tabor, N.J., 2009. Quantitative paleoenvironmental and paleoclimatic reconstruction using paleosols. Earth Sci. Rev. 95, 1–52.

Sickmann, Z.T., Schwartz, T.M., Graham, S.A., 2018. Refining stratigraphy and tectonic history using detrital zircon maximum depositional age: an example from the Cerro Fortaleza Formation, Austral Basin, southern Patagonia. Basin Research 30 (4), 708-729.

Soil Survey Staff, 1999. Soil taxonomy. In: A Basic System of Soil Classification for Making and Interpreting Soil Surveys. US Department of Agriculture, Natural Resource Conservation Service, Washington, D.C, p. 871.

Soil Survey Staff, 2014. Keys to Soil Taxonomy, 12th ed. Washington, DC, USDA-Natural Resources Conservation Service, p. 360.

Song, B., Zhanga, K., Zhanga, L., Ji, J., Hong, H., Wei, Y., Xu, Y., Algeob, T.J., Wang, C., 2018. Qaidam Basin paleosols reflect climate and weathering intensity on the northeastern Tibetan Plateau during the early Eocene Climatic Optimum. Palaeogeogr. Palaeoclimatol. Palaeoecol. 512, 6–22. https://doi.org/10.1016/j. palaeo.2018.03.027.

Srivastava, P., Bhattacharyya, T., Pal, D.K., 2002. Significance of the formation of calcium carbonate minerals in the pedogenesis and management of cracking clay soils (Vertisols) of India. Clays and Clay Minerals, 50, 111-126.

Srivastava, P., Rajak, M.K., Sinha, R., Pal, D.K., Bhattacharyya, T., 2010. A high resolution micromorphological record of the late Quaternary Paleosols from Ganga-Yamuna Interfluve: stratigraphic and paleoclimatic implications. Quat. Int. 227, 127–142.

Stoops, G., 2003. Guidelines for Analysis and Description of Soil and Regolith Thin Sections. Wisconsin, Soil Science Society of America, Madison, p. 184.

Stoops, G., Marcelino, V., Mess, F., 2010. Interpretation of Micromorphological Features of Soils and Regoliths. Elsevier, pp. 720.

Stoops, G., Marcelino, V., Mees, F., 2018. Interpretation of Micromorphological Features of Soils and Regoliths Elsevier, Amsterdam, 2nd ed, p. 1000.

Tabor, N.J., Myers, T.S., Michel, L.A., 2017. Sedimentologist's Guide for Recognition, Description, and Classification of Paleosols. In: Zeigler, K.E., Parker, W.G. (Eds.), Terrestrial Depositional Systems: Deciphering Complexities through Multiple Stratigraphic Methods. Elsevier, Amsterdam, pp. 165–208. https://doi.org/10.1016/ B978-0-12-803243-5.00004-2.

Tettamanti, C., Moyano-Paz, D., Varela, A.N., Tineo, D.E., Gómez-Peral, L.E., Poiré, D.G., Cereceda, A., Odino Barreto, A.L. 2018. Sedimentology and fluvial styles of the Uppermost Cretaceous Continental Deposits of the Austral-Magallanes Basin, Patagonia, Argentina. Latin American Journal of Sedimentology and Basin Analysis 25 (2), 149-168.

Therrien, F., 2005. Palaeoenvironments of the latest Cretaceous (Maastrichtian) dinosaurs of Romania: insights from fluvial deposits and paleosols of the Transylvanian and Haţeg basins. Palaeogeography, Palaeoclimatology, Palaeoecology 218, 15–56.

Therrien, F., Zelenitsky, D.K., Weishampel, D.B., 2009. Palaeoenvironmental reconstruction of the Late Cretaceous Sânpetru Formation (Haţeg Basin, Romania) using paleosols and implications for the "disappearance" of dinosaurs. Palaeogeography, Palaeoclimatology, Palaeoecology, 272, 37-52.

Vajda, V., Bercovici, A., 2012. Pollen and spore stratigraphy of the Cretaceous-Paleogene mass-extinction interval in the Southern Hemisphere. Journal of stratigraphy 36, 154–164.

Van Geel, B., Grenfell, H.R., 1996. Green and Blue-green algae. In: Jansonius, J., McGregor, D.C. (eds.). Palynology: principles and applications. Chapter 7A- Spores of Zygnemataceae. American Association of Stratigraphic Palynologists Foundation 1, 173–179.

van Hinsbergen, D.J.J., de Groot, L.V., van Schaik, S.J., Spakman, W., Bijl, P.K., Sluijs, A., 2015. A paleolatitude calculator for paleoclimate studies. PLoS One 10 (6), e0126946. http://dx.doi.org/10.1371/journal.pone.0126946.

Varela, A.N., Poiré, D.G., Martin, T., Gerdes, A., Goin, F.J., Gelfo, J.N., Hoffmann, S. 2012a. U-Pb zircon constraints on the age of the Cretaceous Mata Amarilla Formation, Southern Patagonia, Argentina: its relationship with the evolution of the Austral Basin. Andean Geology 39 (3), 359-379.

Varela, A.N., Veiga, G.D., Poiré, D.G., 2012b. Sequence stratigraphic analysis of Cenomanian greenhouse palaeosols: a case study from southern Patagonia, Argentina. Sedimentary Geology 271-272, 67–82.

Varela, A.N., Raigemborn, M.S., Richiano, S., White, T., Poiré, D.G., Lizzoli, S. 2018. Late Cretaceous paleosols as paleoclimate proxies of high-latitude Southern Hemisphere: Mata Amarilla Formation, Patagonia, Argentina. Sedimentary Geology 363, 83-95.

Varela, A.N., Yeste, L.M., Viseras, C., García-García, F., Moyano-Paz, D. 2021. Implications of palaeosols in low net-to-gross fluvial architecture reconstruction: Reservoir analogues from Patagonia and Spain. Palaeogeography, Palaeoclimatology, Palaeoecology 577, 110553.

Vepraskas, M.J., 1992. Redoximorphic features for identifying aquic conditions. North Carolina Agriculture Research Service Technical Bulletin 301, 1–33.

Vepraskas, M.J., 1994. Redoximorphic features for identifying aquic conditions. In: Tech. Bull. 301. North Carolina Agric. Res. Serv., North Carolina State Univ., Raleigh.

Vepraskas, M. J., 1995 (revised). Redoximorphic Features for Identifying Aquic Conditions. Technical Bulletin 301, North Carolina State University, Raleigh, NC.

Vepraskas, M.J., 2015. Redoximorphic Features for Identifying Aquic Conditions: North Carolina State University. College of Agriculture and Life Sciences, p. 30.

Vepraskas, M.J., Craft, C.B., 2016. Wetland Soils: Genesis, Hydrology, Landscapes, and Classification; CRC Press: Boca Raton, FL, USA.

Vepraskas, M.J., Lindbo, D.L., Stolt, M.H., 2018. Redoximorphic Features. In: Stoops, G., Marcelino, V., Mees, F. (Eds.). Interpretation of Micromorphological Features of Soils and Regoliths (Second Edition), Elsevier, pp. 425-445.

Vera, E.I., Pérez Loinaze, V.S., Moyano-Paz, D., Coronel, M.D., Manabe, M., Tsuihiji, T., Novas, F.E. 2022. Paleobotany of the uppermost Cretaceous Chorrillo Formation, Santa Cruz province, Argentina. Insights in a freshwater floral community. Cretaceous Research 138, 105296.

Volkheimer,W., Scafati, L., Melendi, D.L., 2007. Palynology of a Danian warm climatic wetland in Central Northern Patagonia, Argentina. Revista Española de Micropaleontología 39, 117–134.

Wilson, M.J., 1999. The origin and formation of clay minerals in soils: past, present and future perspectives. Clay minerals, 34(1), 7-25.

Wright, V.P., Taylor, K.G., Beck, V.H., 2000. The paleohydrology of Lower Cretaceous seasonal wetlands, Isle of Wight, southern England. Journal of Sedimentary Research 70, 619–632.

Yeste, L.M., Varela, A.N., Viseras, C., McDougall, N., García-García, F., 2020. Reservoir architecture and heterogeneity distribution in floodplain sandstones: key features in outcrop, core and wireline logs. Sedimentology 67, 3355–3388.

Zippi, P., 1998. Freshwater algae from the Mattagami Formation (Albian), Ontario: Paleoecology, botanical affinities, and systematic taxonomy. Micropaleontology, Suppl. 1, 44, 1–78.

Captions

TABLES

TABLE 1: Macro and micropedofeatures, clay mineralogy and main pedological processes in the paleosols of the Chorrillo Formation

TABLE 2: X-ray Diffraction data of the paleosols of the Chorrillo Formation

FIGURES

FIGURE 1: A. Location map of the Austral-Magallanes Basin. LAR = Lago Argentino región; UER = Última Esperanza región. B. Stratigraphic scheme of the Upper Cretaceous Units of the Lago Argentino region. C. Geological map showing the distribution of the Upper Cretaceous units south of Lago Argentino. CT = Cerro Toro; AV = Alta Vista; CF = Cerro Fortaleza; LI = La Irene; MA = Man Aike.

FIGURE 2: Sedimentary measured section of the Chorrillo Formation showing main sedimentological aspects, paleosol bearing levels with typical pedofeatures and the location of the fossil content.

FIGURE 3: A: General appearance of the middle section of the Chorrillo Formation in the La Anita area. White arrows indicate the pedogenized profiles of Argentino Lake pedotype. The white circle indicate a person for scale. B: Representative profile and clay mineralogy (S: smectite; I: Illite; C: Chlorite; IS: mixed layers of illite-smectite; K: kaolinite) of the Argentino Lake pedotype. See position and key of Fig. 2 for macrofeatures; scale bar = 0.35 m. C: Bssg horizon with slickensides that define angular blocky peds. D: Subangular blocky peds with olive yellow (white arrows) and light greenish gray (white dotted lines) mottles in a Bssg horizon. E: Micromass of ABss horizon mainly formed of clays impregnated with of Fe/Mn oxides. Note the subangular blocky microstructure defined by planar voids (PPL). F: Micromass of a Bssg horizon with parallel-striated b-fabric. Note abundant Fe-nodules surrounded by depletion zones (XPL). G: Bssg horizon with a blocky microstructure defined by planar voids (PPL). Scale bars in E–G = 100 micrometers. PPL: plane polarized light; XPL: cross polarized light.

FIGURE 4: A: General appearance of the entire Chorrillo Formation in the La Anita area. White arrow indicates the pedogenized profiles of Perito Moreno Glacier pedotype in the

lower part of the middle section of the unit. The white circle indicate a person for scale. B: Representative profile and clay mineralogy (S: smectite; I: Illite; C: Chlorite; IS: mixed layers of illite-smectite; K: kaolinite) of the Perito Moreno Glacier pedotype. See position and key of Fig. 2 for macrofeatures; scale bar = 0.35 m.. C: Bssk horizon with coalescent carbonatic-nodules with a diameter of 300 mm (note hammer for scale). D: Bssk horizon with slickensides that define angular blocky peds and a mottle indicated with a white arrow. E: Micromass of a carbonate-nodule composed of micritic calcite with impregnated Fe/Mn-zones (XPL). F: Micromass of a Bssk horizon with depletion zones (PPL). G: Cross- and grano-striated b-fabric in Bssk horizon (XPL). Scale bars in E–G = 100 micrometers. PPL: plane polarized light; XPL: cross polarized light.

FIGURE 5: A: General appearance of the entire Chorrillo Formation in the La Anita area. White arrow indicates the pedogenized profiles of Anita Farm pedotype in the middle section of the unit. The white circle indicate a person for scale. B: Representative profile and clay mineralogy (S: smectite; I: Illite; IS: mixed layers of illite-smectite) of the Anita Farm pedotype. See position and key of Fig. 2 for macrofeatures; scale bar = 0.35 m. C: Field photograph of a Bssg horizon. D: Detail of a Bssg horizon ped with yellow mottles. E: Micromass of a Bssg horizon with incipient grano-striated b-fabric (XPL). F: Abundant planar voids and channels that defined an angular–subangular blocky microstructure. Note also Fe-hypocoatings and depletion zones (PPL). G: Micromass of a Bssg horizon with channels (XPL). Scale bars in E–G = 100 micrometers. PPL: plane polarized light; XPL: cross polarized light.

FIGURE 6: A: General appearance of the entire section of the Chorrillo Formation in the La Anita area. White arrow indicates the pedogenized profiles of Centinela River pedotype in

the lower section of the unit. The white circle indicate a person for scale. B: Representative profile and clay mineralogy (S: smectite; I: Illite; C: Chlorite) of the Centinela River pedotype. See position and key of Fig. 2 for macrofeatures; scale bar = 0.35 m. C: Very coarse platy peds of an Oa horizon. Note the black carbonized organic matter and remains of leaves and fibers (white arrows). D: Coarse yellow red rhizoliths in an ABg horizon. E: Micromass of an Oa horizon with abundant carbonaceous remains (PPL, x10). F: Micromass of an ABg horizon with clays impregnated with Fe/Mn oxides. Note the subangular blocky microstructure defined by channels and chambers (PPL). G: Micromass of a Bg horizon mainly formed of clays impregnated with Fe/Mn oxides and a channel with a depletion zone around (PPL). Scale bars in E–G = 100 micrometers. PPL: plane polarized light; XPL: cross polarized light.

FIGURE 7: A: General appearance of the upper section of the Chorrillo Formation in the La Anita area. White arrow indicates the pedogenized profiles of Chorrillo Malo Farm pedotype. The white circle indicate a person for scale. B: Representative profile and clay mineralogy (S: smectite; I: Illite; C: Chlorite; K: kaolinite) of the Chorrillo Malo Farm pedotype. See position and key of Fig. 2 for macrofeatures; scale bar = 0.35 m. C: Subangular blocky peds in a Bss horizon. D–E: Bss horizon with a typic Fe- and clay coating associated with a depletion zone (XPL). Scale bars in E–F = 100 micrometers. PPL: plane polarized light; XPL: cross polarized light.

FIGURE 8: Schematic reconstruction of the paleoenvironmental interpretation and evolution of the Chorrillo Formation paleosols. Flora illustrated on these reconstructed landscapes are based on paleoflora reported from the unit (see the text for explanation).

Table 1: Macro and micropedofeatures, clay mineralogy and main pedological processes in the paleosols of the Chorrillo Formation

Pedotype	Hz.	Macropedofeatures	Micropedofeatures	Clay mineralogy	Pedogenic processes
Argentino Lake pedotype – moderatelly-developed hydromorphic Vertisols	ABss	Rhizoliths (B); rhizohalos (H); slickensides	Fe-nodules and depletion zones (H); pedorelicts	S (100–80%; V); I and/or C (5–10%); IS and/or K (5%)	Vertization (V) > hydromorphism (H) > Bioturbation (B)
	Bssg	Slickensides (V); rhizoliths (B); rhizohalos and mottles (H)	Fe-nodules and - mottles and depletion zones (H)	S (100–60%; V); I and/or C (5–20%); IS and/or K (5%)	
Perito Moreno Glacier pedotype – calcic Vertisols	ABssg	Rhizoliths (B); rhizohalos, mottles and Fe-nodules (H)	Fe-nodules and depletion zones (H); pedorelicts	S (65–80%; V); I (10–30%); IS (5-10%); C (<15%)	Vertization (V) > calcification (C) > hydromorphism (H) > Bioturbation (B)
	Bssk	Carbonate-nodules (C); Rhizoliths (B); rhizohalos and mottles (H); slickensides (V)	Cabonate-nodules (C); depletion zones (H); pedorelicts	S (60–95%; V); I (5–20%); IS and C (>5%); K (<15%)	
	Ck	Mottles (H); powdery carbonate (C)	-	S (70–95%; V); I (5–15%); IS and C (>5%); K (<5%)	
Anita Farm pedotype – poorly-developed hydromorphic Protosols	Bssg	Mottles (H); Rhizoliths (B); Slickensides (V)	Fe-nodules and - hypocoatings, and depletion zones (H)	S (100–80%; V); I, IS and/or K (5–10%)	Hydromorphism (H) > Vertization (V) > Bioturbation (B)
	C	Mottles (H)	-	S (95–90%; V); I, IS (<5%)	
Centinela River pedotype – Histosols	Oa	Rhizoliths (B); Rhizohalos (H)	Fe-nodules and - hypocoatings (H)	S (65–80%; V); C (10–20%); I (10%)	Hydromorphism (H) > Bioturbation (B) > Vertization (V)
	ABg	Rhizoliths (B); mottles (H)	Fe-nodules and - hypocoatings (H)	S (85%; V); I (15%)	
	Bg	Rhizoliths (B); mottles (H); slickensides (V)	Fe-nodules and depletion zones (H)	S (90-100%; V); C (10%)	
Chorrillo Malo Farm pedotype – argillic Vertisols	Bss	Rhizoliths (B); rhizohalos (H)	Clay-coatings (I); Fe-coatings and depletion zones (H)	S (60%; V); I (30%); C and K (5%)	Illuviation (I) > Bioturbation (B) > Vertization (V) > Hydromorphism (H)

Table 2: X-ray Diffraction data of the paleosols of the Chorrillo Formation

Sample	Pedotype	Horizon	Whole Rock					Clay fraction					
			Q	FK	Pl	Clays	Other	I	Sm	Sm Cr	IS	Cl	K
PCH-18-4	CMF	Bw	va	t	s	m	vs	30	60	g	0	5	5
PCH-18-3	AL	ABss	va	vs	s	a	vs	10	80	g	0	5	5
PCH-18-2	AL	Bssg	va	t	s	m	vs	10	90	r	0	0	0
PCH-18-1	AF	Bssg	va	t	s	m	vs	10	85	b	5	0	0
PCH-17-5	AL	Bssg	s	vs	m	va	vs	5	90	vg	0	5	0
PCH-17-4	AL	Bssg	va	vs	s	a	vs	20	70	g	0	5	5
PCH-17-3- K	PMG	Bssk nodule	vs	-	t	vs	vs	0	100	b	0	0	0
PCH-17-2-M	PMG	Bssk	va	vs	vs	a	vs	15	80	r	5	0	0
PCH-17-2- K	PMG	Bssk nodule	a	-	t	s	vs	5	95	r	0	0	0
PCH-17-1	PMG	ABssg	va	t	vs	a	vs	30	65	b	5	0	0
PCH-16-9	PMG	ABssg	va	t	s	s	vs	20	70	b	10	0	0
PCH-16-8- K	PMG	Bssk nodule	a	t	vs	vs	vs	15	80	b	5	0	0
PCH-16-7- K	PMG	Bssk nodule	s	-	vs	vs	vs	10	80	b	5	t	5
PCH-16-6- K	PMG	Bssk nodule	a	t	vs	vs	vs	15	60	r	5	5	15
PCH-16-5- K	PMG	Bssk nodule	a	t	vs	s	vs	15	60	r	5	5	15
PCH-16-3	PMG	Bssk	va	t	m	s	vs	20	60	r	0	5	15
PCH-16-2-K	PMG	C nodule	a	vs	s	s	vs	10	65	r	5	10	10
PCH-16-2-M	PMG	C	va	vs	m	s	vs	15	70	b	5	5	5
PCH-16-1	AL	Bssg	va	vs	s	m	vs	15	80	b	5	0	0
PCH-15-2	AF	Bssg	va	t	vs	a	vs	0	100	b	0	0	0
PCH-15-1	AF	Bssg	va	t	m	m	vs	5	90	b	0	5	0
PCH-15-0	AF	C	va	t	s	a	vs	5	95	b	0	0	0
PCH-14-2	CR	Oa	va	t	s	s	vs	15	65	r	0	20	0
PCH-14-1	CR	Bg	va	t	s	m	vs	0	90	g	0	10	0
PCH-14-0	CR	Bg	va	t	m	m	vs	0	100	g	0	0	0
PCH-12-3	AL	Bssg	va	vs	s	m	vs	10	90	r	0	0	0
PCH-12-2	AL	ABss	va	t	m	s	vs	10	80	g	0	10	0
PCH-12-1	AL	Bssg	va	t	s	a	vs	10	85	vg	0	5	0
PCH-10-3-k	PMG	Bssk nodule	s	t	vs	s	vs	0	100	b	0	0	0
PCH-10-2	PMG	ABssg	va	t	s	m	vs	10	70	r	5	15	0
PCH-10-1	AL	Bssg	va	vs	s	s	vs	30	60	b	0	10	0

PCH-9-7	CR	Oa	va	t	s	m	vs	10	80	g	0	10	0
PCH-9-6	CR	ABg	va	t	s	m	vs	15	85	g	0	0	0
PCH-9-6-riz	CR	ABg rizolith	va	t	vs	s	vs	15	85	b	0	0	0
PCH-9-5	AF	Bssg	va	vs	s	m	vs	0	100	g	0	0	0
PCH-9-4-K	PMG	Bssk nodule	s	-	vs	vs	vs	0	100	r	0	0	0
PCH-9-4-M	PMG	Bssk	va	t	s	a	vs	5	95	g	0	0	0
PCH-9-3-K	PMG	Bssk nodule	s	t	vs	vs	vs	0	100	r	0	0	0
PCH-9-3-M	PMG	Bssk	va	t	s	m	vs	5	90	b	5	0	0
PCH-16-3-C	PMG	C	va	t	m	s	vs	5	95	b	0	0	0

Table 2: Continued

	Pedotype	Horizon	Whole Rock					Clay fraction					
			Q	FK	Pl	Clays	Other	I	Sm	Sm Cr	IS	Cl	K
PCH-9-2	PMG	ABssg	va	t	s	m	vs	15	80	b	5	0	0
PCH-9-1-K	PMG	Bssk nodule	s	-	t	vs	vs	0	100	g	0	0	0
PCH-9-1-M	PMG	Bssk	va	vs	s	s	vs	5	90	b	5	0	0
PCH-8-7-K	PMG	Bssk nodule	s	t	vs	vs	vs	0	100	b	0	0	0
PCH-8-5	AL	Bssg	va	t	s	m	vs	5	95	g	0	0	0
PCH-8-4	AL	Bssg	va	vs	s	m	vs	0	100	r	0	0	0
PCH-8-3	AL	ABss	va	vs	s	s	vs	5	85	g	0	5	5
PCH-8-2	AL	Bssg	va	t	s	s	vs	0	90	g	0	10	0
PCH-8-1	AL	Bssg	va	t	s	m	vs	20	60	r	0	15	5
PCH-7-2	AL	Bssg	va	vs	vs	a	vs	5	90	b	5	0	0
PCH-7-1	AL	ABss	va	t	s	a	vs	10	85	r	5	0	0
PCH-5-4	AL	Bssg	va	t	s	m	vs	10	75	b	5	5	5
PCH-5-3	AL	Bssg	va	t	m	m	vs	10	80	g	0	5	5
PCH-4-3	AL	ABss	va	vs	s	a	vs	0	100	vg	0	0	0
PCH-4-2	AL	Bssg	a	t	s	va	vs	10	85	vg	0	5	0
PCH-4-1	AL	Bssg	va	vs	s	m	vs	10	80	r	0	10	0
PCH-1-4	AF	Bssg	va	t	s	a	vs	10	85	b	5	0	0
PCH-1-3	AF	C	va	t	s	a	vs	5	90	b	5	0	0
PCH-1-2	AL	Bssg	va	t	vs	m	vs	10	85	b	5	0	0
PCH-1-1	AL	Bssg	va	-	vs	m	vs	15	75	b	5	0	5

Abbreviations: AL = Argentino Lake pedotype, PMG = Perito Moreno Glacier pedotype, AF = Anita Farm pedotype, CR = Centinela River pedotype, CMF = Chorrillo Malo Farm pedotype, Q = quartz, FK = potassium feldspar, Pl = plagioclase, I = illite, Sm = smectite, Cr =crystallinity, IS = mixed layers of illite-smectite, Cl = chlorite, K = kaolinite, va = very abundant, a = abundant, m = moderate, s = scarce, vs = very scarce, t = trace, - = no data, vg = very good, g = good, r = regular, b = bad

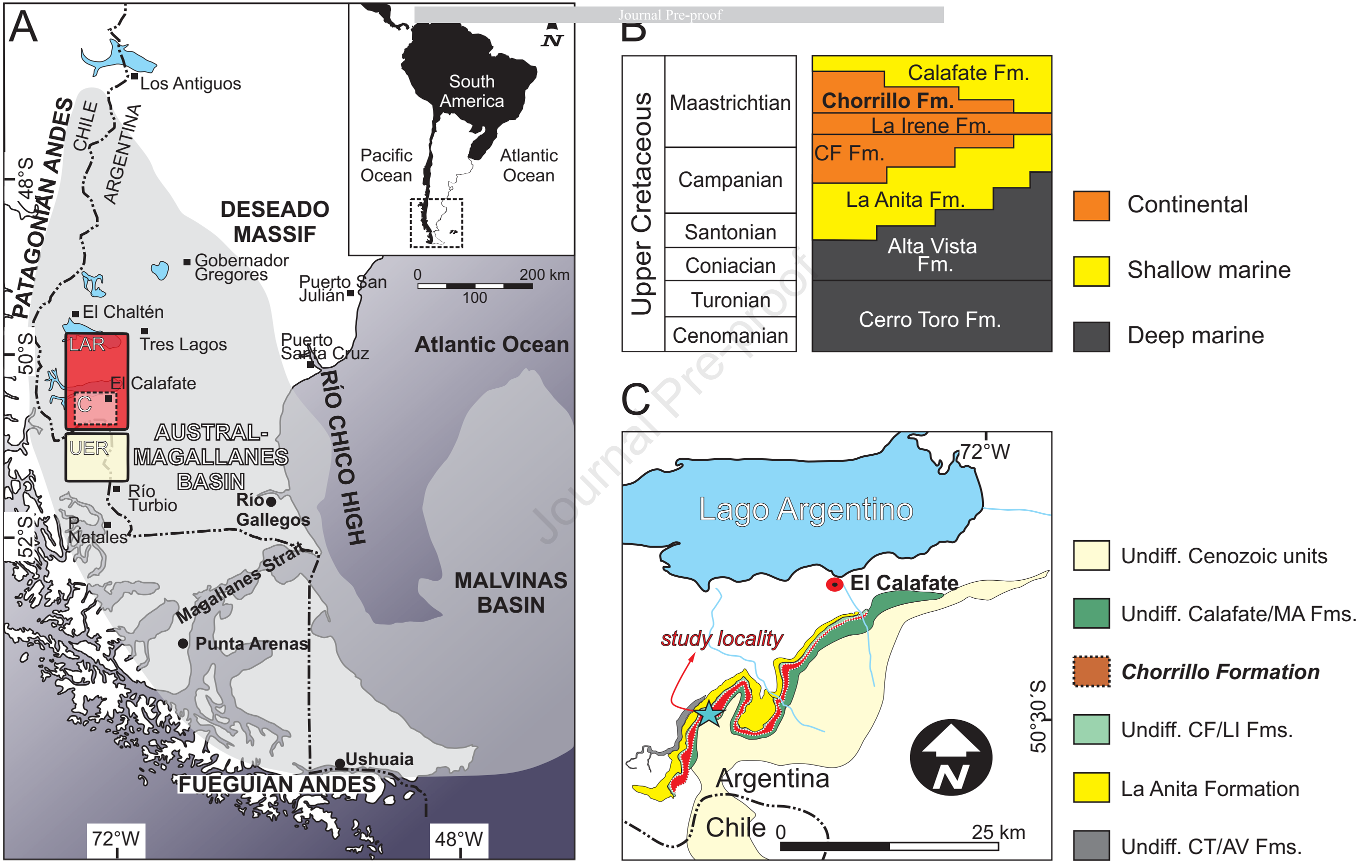
A
Los Antiguos
PATAGONIAN ANDES
CHILE
ARGENTINA
48°S
DESEADO
MASSIF
Gobernador
Gregores
Puerto San
Julián
El Chaltén
Tres Lagos
Puerto
Santa Cruz
LAR
El Calafate
C
50°S
AUSTRAL-
MAGALLANES
BASIN
UER
Río
Turbio
Río
Gallegos
P.
Natales
52°S
RÍO CHICO HIGH
Atlantic Ocean
MALVINAS
BASIN
Magallanes Strait
Punta Arenas
Ushuaia
FUEGUIAN ANDES
72°W
48°W
South
America
Pacific
Ocean
Atlantic
Ocean
N
0
100
200 km
B
Upper Cretaceous
Maastrichtian
Campanian
Santonian
Coniacian
Turonian
Cenomanian
Calafate Fm.
Chorrillo Fm.
La Irene Fm.
CF Fm.
La Anita Fm.
Alta Vista
Fm.
Cerro Toro Fm.
Continental
Shallow marine
Deep marine
C
72°W
Lago Argentino
El Calafate
study locality
50°30´S
Argentina
Chile
0
25 km
N
Undiff. Cenozoic units
Undiff. Calafate/MA Fms.
Chorrillo Formation
Undiff. CF/LI Fms.
La Anita Formation
Undiff. CT/AV Fms.

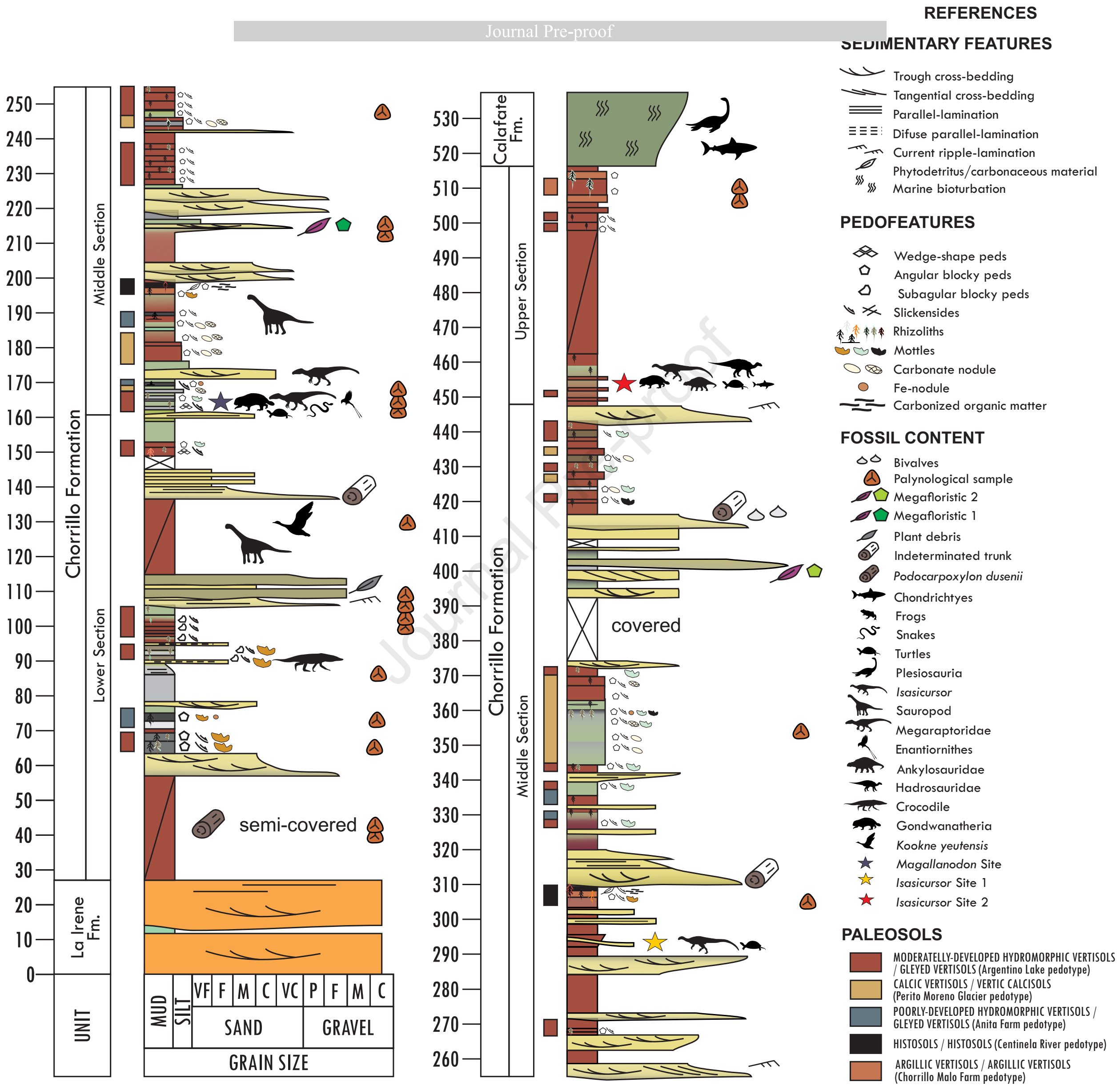
REFERENCES
SEDIMENTARY FEATURES
Trough cross-bedding
Tangential cross-bedding
Parallel-lamination
Difuse parallel-lamination
Current ripple-lamination
Phytodetritus/carbonaceous material
Marine bioturbation
PEDOFEATURES
Wedge-shape peds
Angular blocky peds
Subagular blocky peds
Slickensides
Rhizoliths
Mottles
Carbonate nodule
Fe-nodule
Carbonized organic matter
FOSSIL CONTENT
Bivalves
Palynological sample
Megafloristic 2
Megafloristic 1
Plant debris
Indeterminated trunk
Podocarpoxylon dusenii
Chondrichtyes
Frogs
Snakes
Turtles
Plesiosauria
Isasicursor
Sauropod
Megaraptoridae
Enantiornithes
Ankylosauridae
Hadrosauridae
Crocodile
Gondwanatheria
Kookne yeutensis
Magallanodon Site
Isasicursor Site 1
Isasicursor Site 2
PALEOSOLS
MODERATELLY-DEVELOPED HYDROMORPHIC VERTISOLS / GLEYED VERTISOLS (Argentino Lake pedotype)
CALCIC VERTISOLS / VERTIC CALCISOLS (Perito Moreno Glacier pedotype)
POORLY-DEVELOPED HYDROMORPHIC VERTISOLS / GLEYED VERTISOLS (Anita Farm pedotype)
HISTOSOLS / HISTOSOLS (Centinela River pedotype)
ARGILLIC VERTISOLS / ARGILLIC VERTISOLS (Chorrillo Malo Farm pedotype)
UNIT
La Irene Fm.
Chorrillo Formation
Lower Section
Middle Section
Upper Section
Calafate Fm.
MUD
SILT
VF F M C VC
SAND
P F M C
GRAVEL
GRAIN SIZE
semi-covered
covered
0 10 20 30 40 50 60 70 80 90 100 110 120 130 140 150 160 170 180 190 200 210 220 230 240 250
260 270 280 290 300 310 320 330 340 350 360 370 380 390 400 410 420 430 440 450 460 470 480 490 500 510 520 530

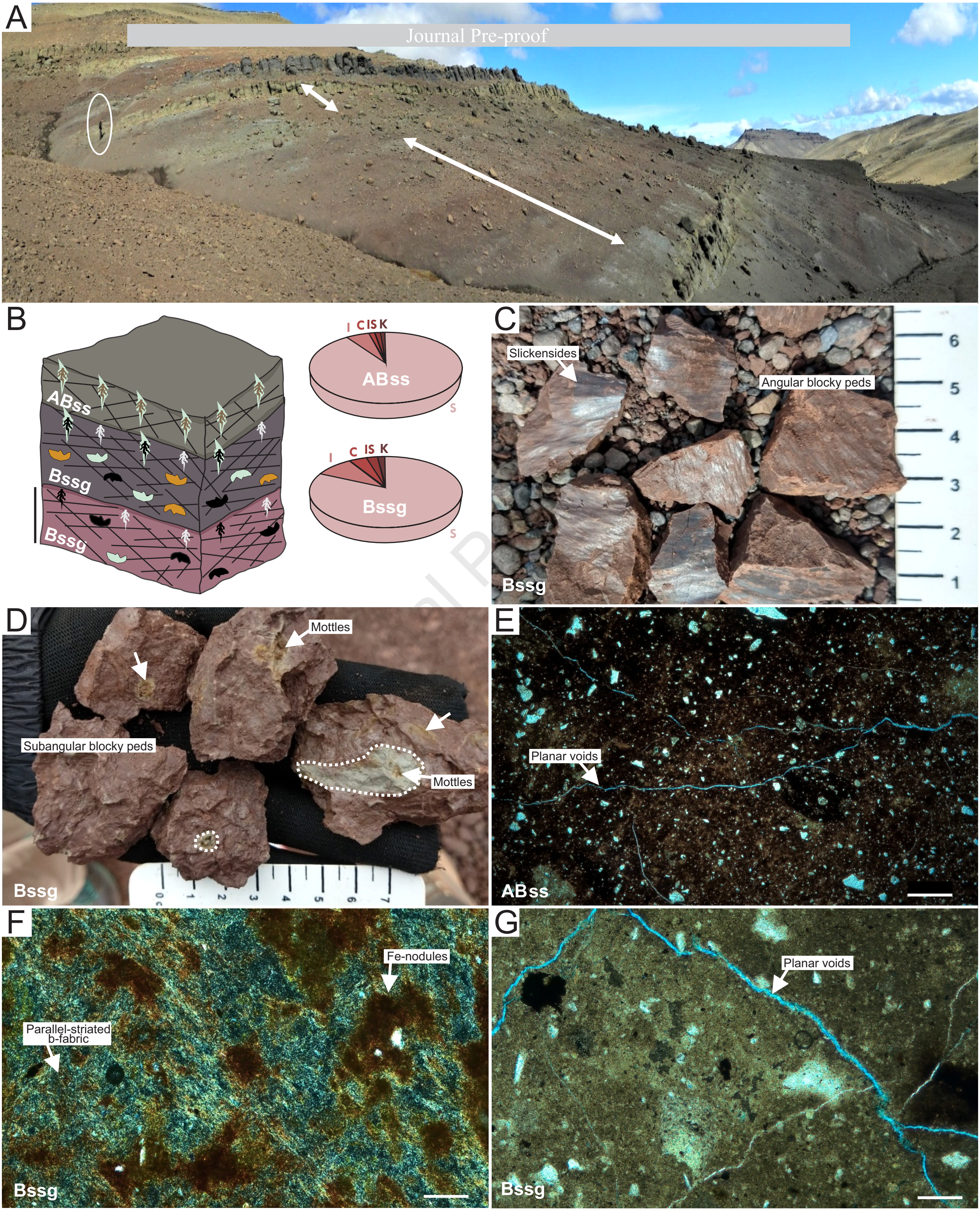
A
B
ABss
Bssg
Bssg
I
C
IS
K
ABss
S
I
C
IS
K
Bssg
S
C
Slickensides
Angular blocky peds
Bssg
D
Mottles
Subangular blocky peds
Mottles
Bssg
E
Planar voids
ABss
F
Fe-nodules
Parallel-striated b-fabric
Bssg
G
Planar voids
Bssg

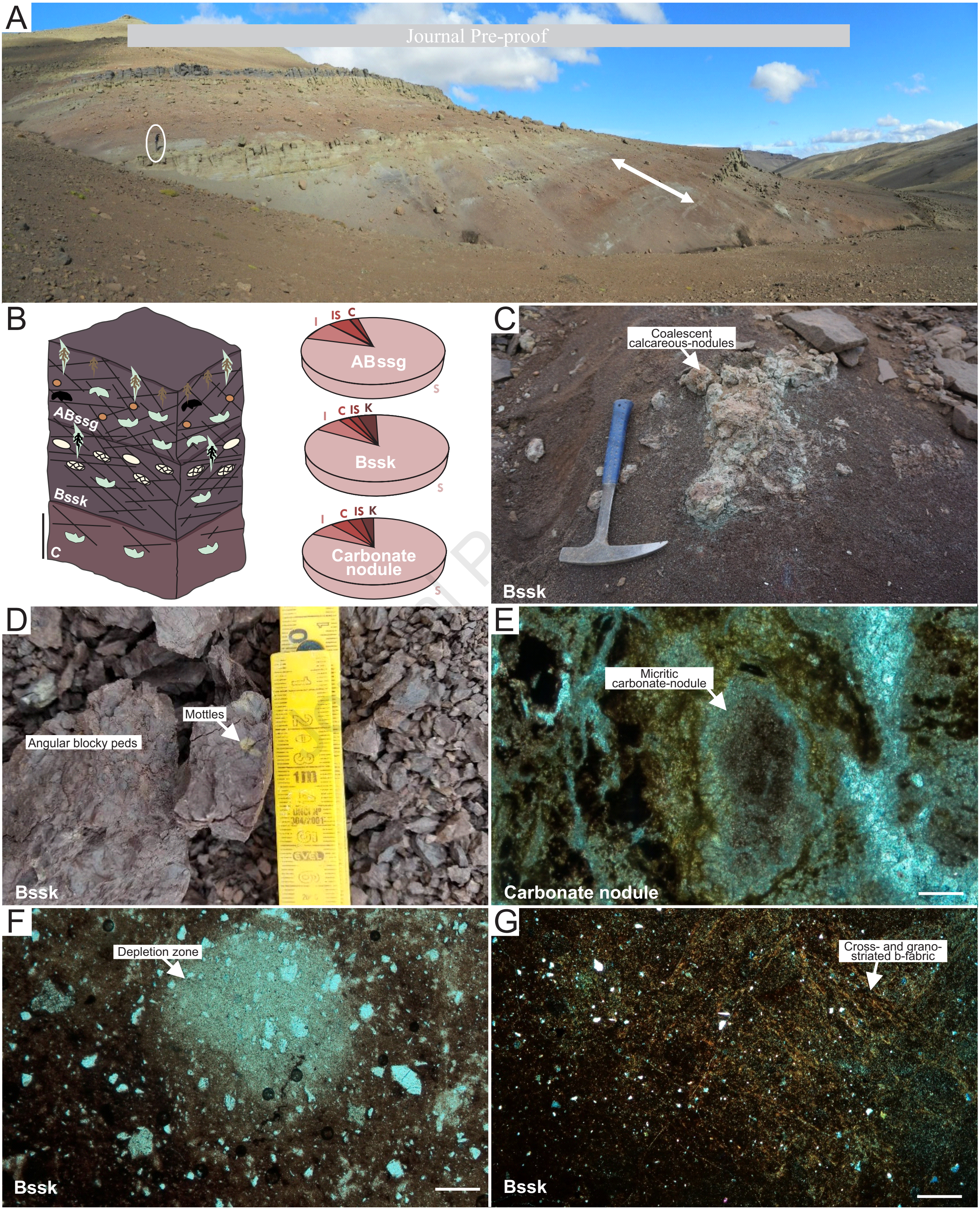
A
B
ABssg
Bssk
C
I
IS
C
K
S
ABssg
Bssk
Carbonate nodule
Coalescent calcareous-nodules
Bssk
D
Angular blocky peds
Mottles
Bssk
E
Micritic carbonate-nodule
Carbonate nodule
F
Depletion zone
Bssk
G
Cross- and grano-striated b-fabric
Bssk

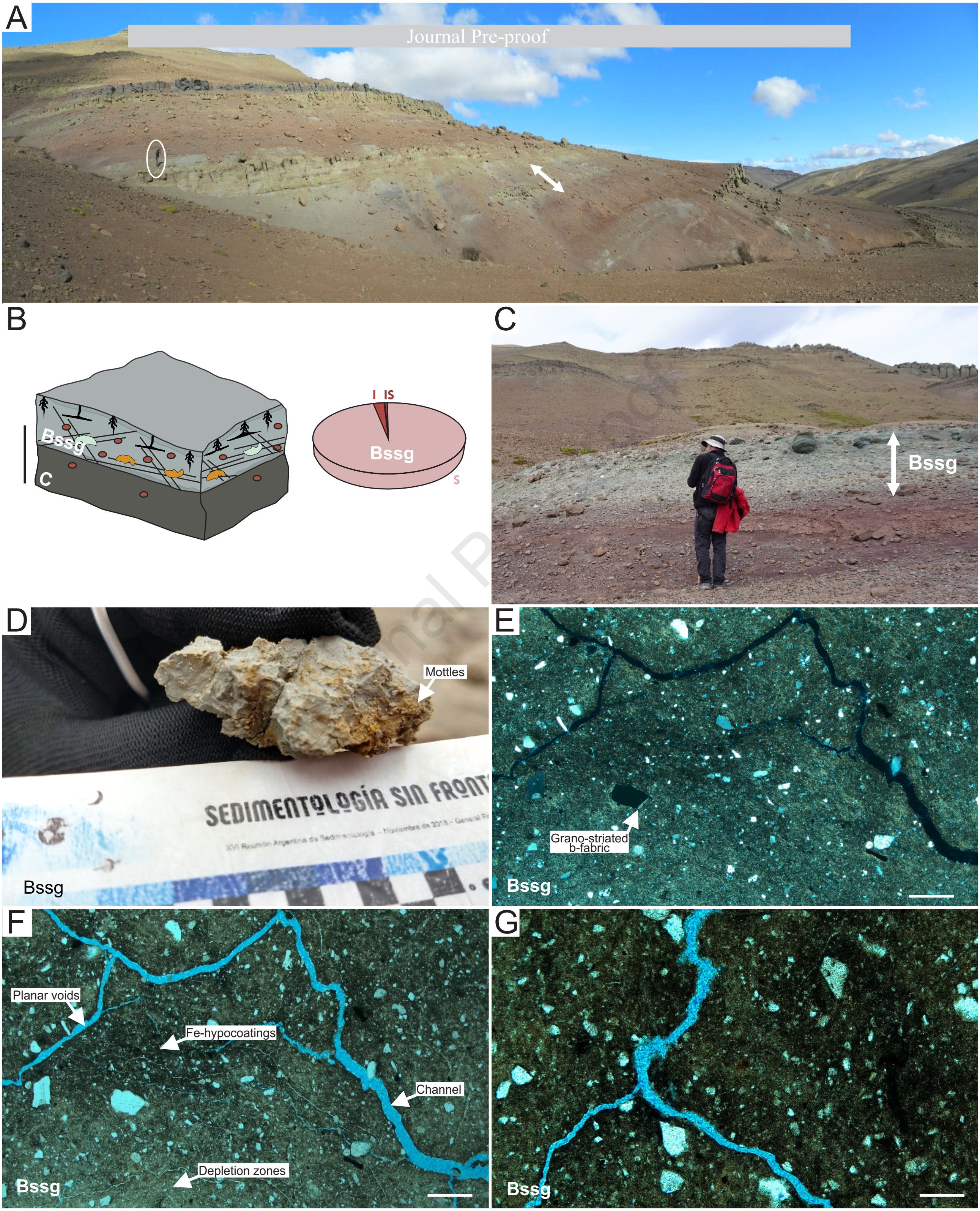
A
B
Bssg
C
I
IS
Bssg
S
C
Bssg
D
Mottles
Bssg
E
Grano-striated
b-fabric
Bssg
F
Planar voids
Fe-hypocoatings
Channel
Depletion zones
Bssg
G
Bssg

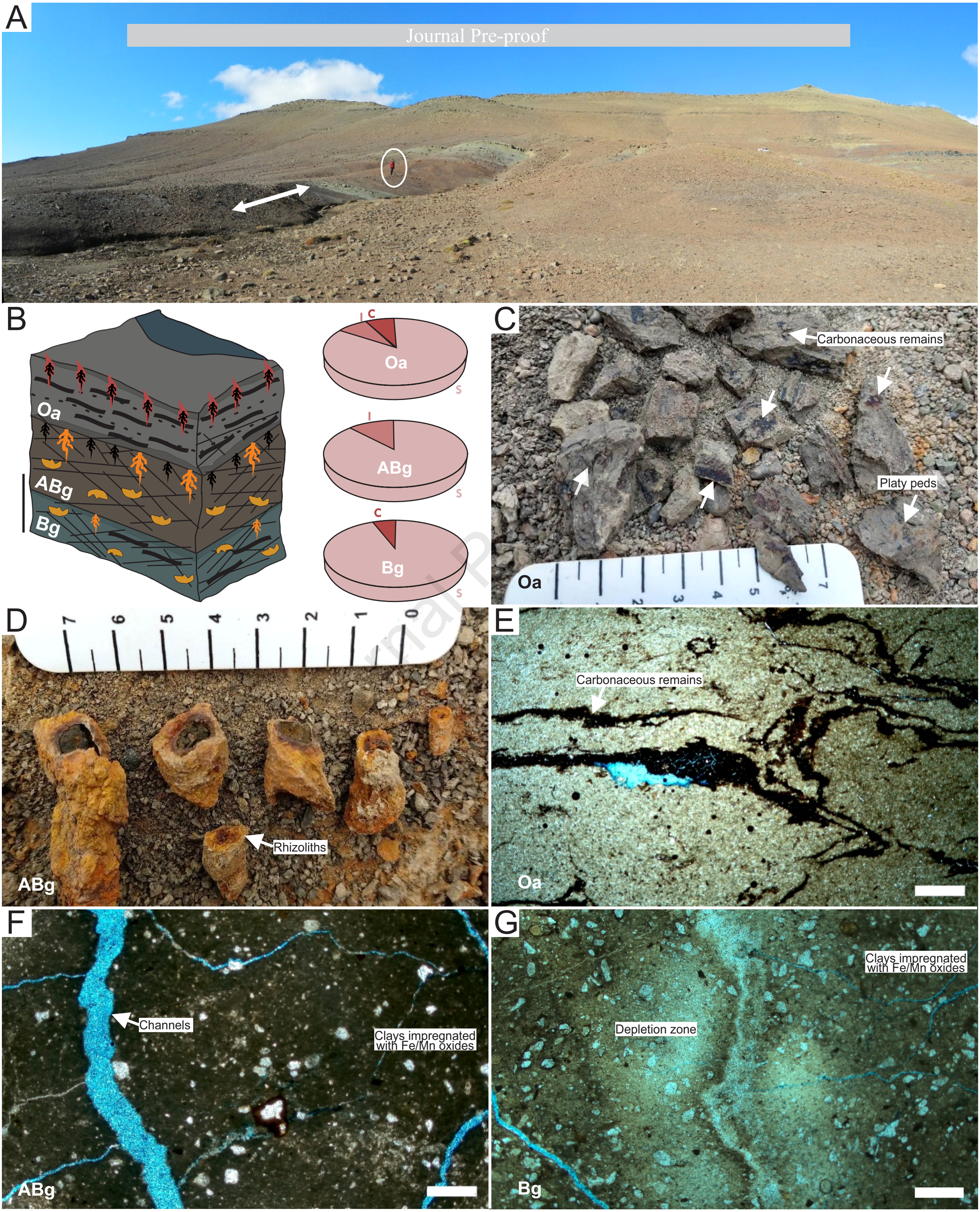
A
B
Oa
ABg
Bg
C
I
S
C
Carbonaceous remains
Platy peds
Oa
D
Rhizoliths
ABg
E
Carbonaceous remains
Oa
F
Channels
Clays impregnated with Fe/Mn oxides
ABg
G
Clays impregnated with Fe/Mn oxides
Depletion zone
Bg

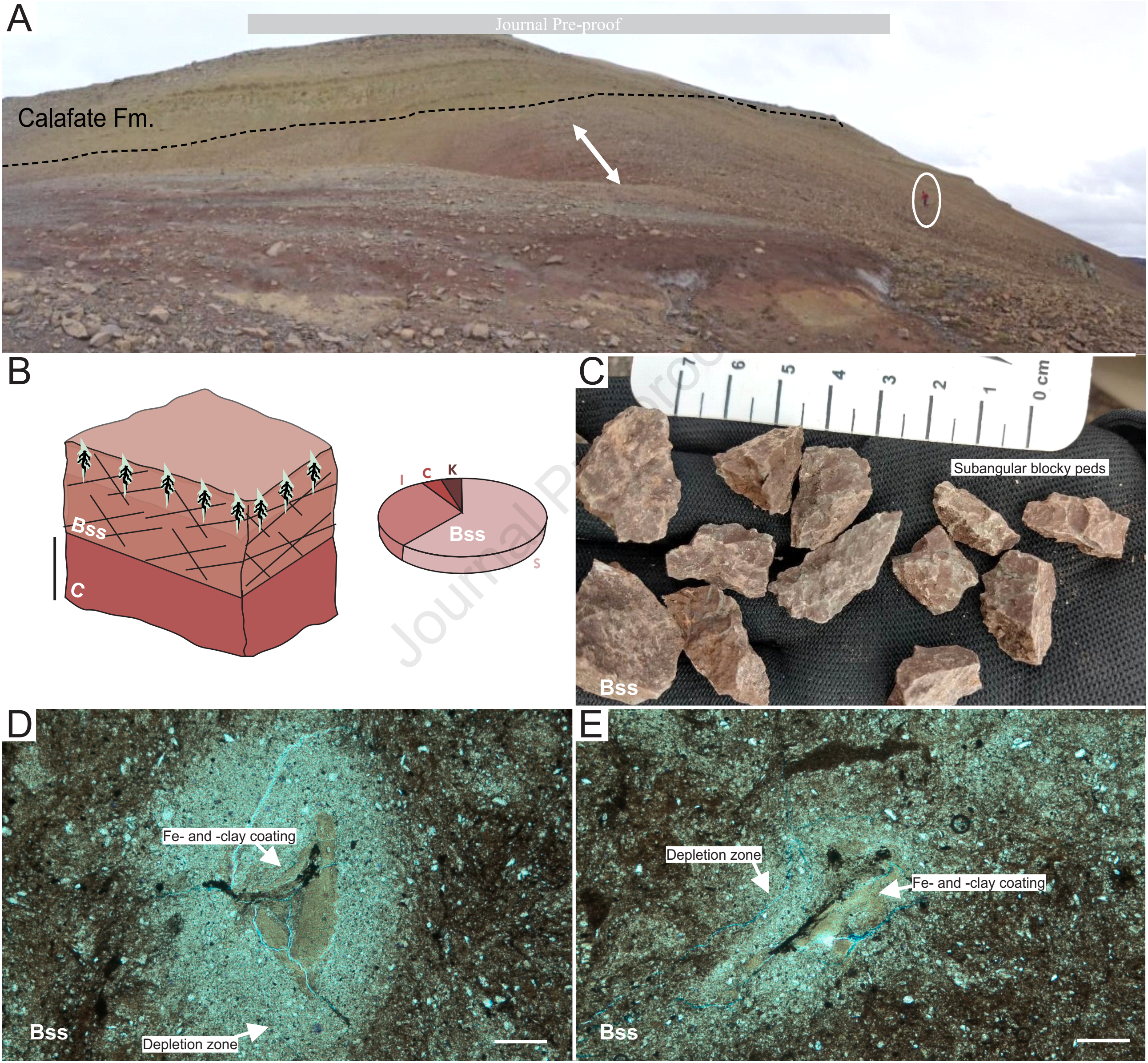
A
Calafate Fm.
B
Bss
C
I
C
K
Bss
S
C
Subangular blocky peds
7
6
5
4
3
2
1
0 cm
Bss
D
Fe- and -clay coating
Bss
Depletion zone
E
Depletion zone
Fe- and -clay coating
Bss

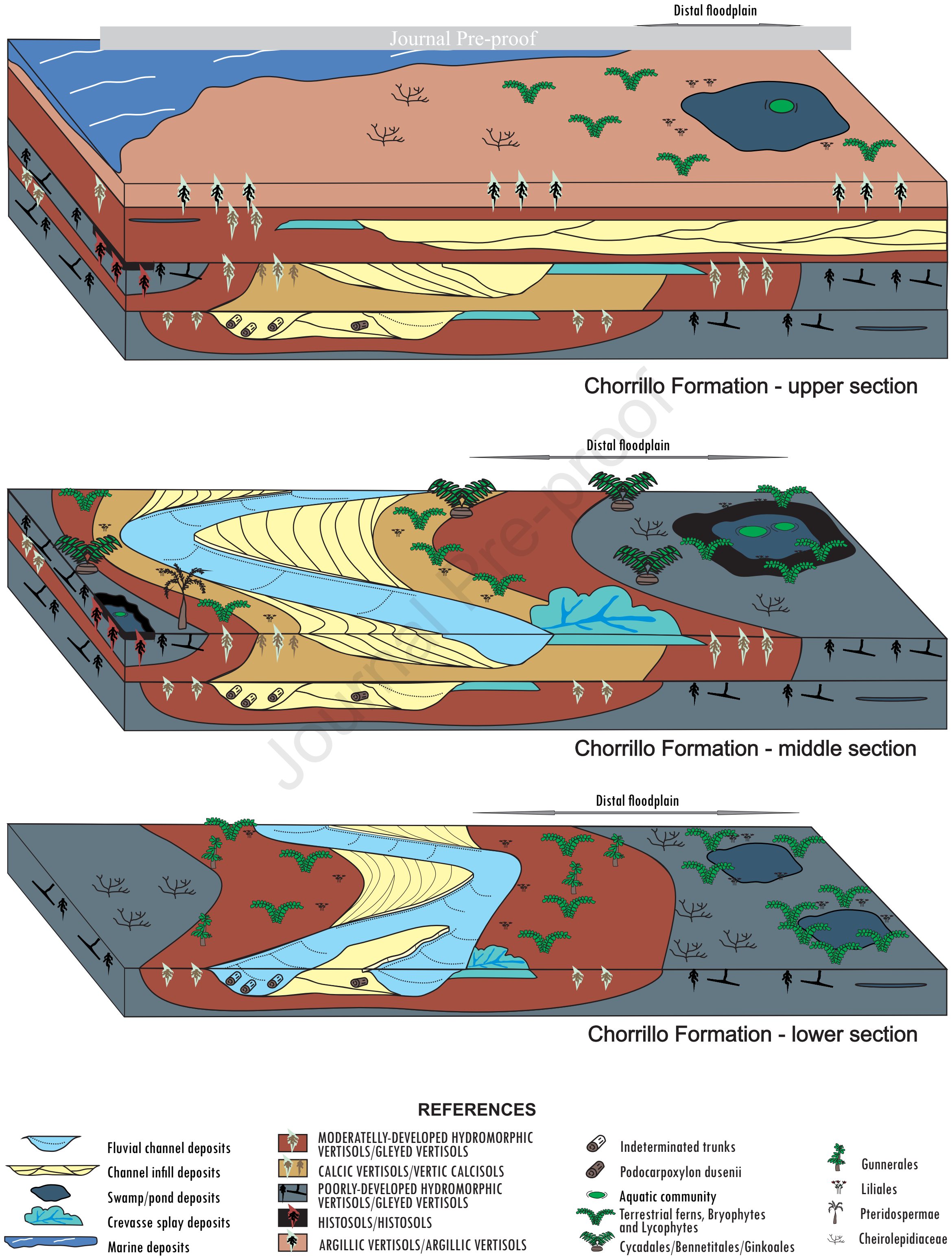
Distal floodplain
Chorrillo Formation - upper section
Distal floodplain
Chorrillo Formation - middle section
Distal floodplain
Chorrillo Formation - lower section
REFERENCES
Fluvial channel deposits
Channel infill deposits
Swamp/pond deposits
Crevasse splay deposits
Marine deposits
MODERATELLY-DEVELOPED HYDROMORPHIC VERTISOLS/GLEYED VERTISOLS
CALCIC VERTISOLS/VERTIC CALCISOLS
POORLY-DEVELOPED HYDROMORPHIC VERTISOLS/GLEYED VERTISOLS
HISTOSOLS/HISTOSOLS
ARGILLIC VERTISOLS/ARGILLIC VERTISOLS
Indeterminated trunks
Podocarpoxylon dusenii
Aquatic community
Terrestrial ferns, Bryophytes and Lycophytes
Cycadales/Bennetitales/Ginkoales
Gunnerales
Liliales
Pteridospermae
Cheirolepidiaceae

Highlights

- Fluvial sediments in southern Patagonia preserve Maastrichtian paleosols
- Stacked hydromorphic, calcic and argillic Vertisols, and Histosols
- Paleosols spatial distribution within the floodplain linked to different location
- Vertical stacking of paleosols linked to avulsion processes
- Maastrichtian paleosols show temperate–warm and seasonally humid climate for mid–high south paleolatitudes

M.S. Raigemborn: Conceptualization, Methodology, Investigation, Writing – Original Draft, Visualization, Resources, Project Administration, Founding acquisition.

S. Lizzoli: Conceptualization, Methodology, Investigation, Writing – Original Draft.

D. Moyano-Paz: Conceptualization, Validation, Writing – Original Draft, Review & Editing.

A. Varela: Conceptualization, Methodology, Validation, Writing – Original Draft, Review & Editing.

D. Poiré: Conceptualization, Methodology, Writing – Original Draf.

V. Perez Loinaze: Writing – Original Draf, Review & Editing.

E. Vera: Writing – Original Draf, Review & Editing.

M. Manabe: Resources, Project Administration, Founding acquisition

F. Novas: Conceptualization, Methodology, Validation, Writing – Original Draft, Review & Editing, Resources, Project Administration, Founding acquisition

Declaration of interests

☒ The authors declare that they have no known competing financial interests or personal relationships that could have appeared to influence the work reported in this paper.

☐The authors declare the following financial interests/personal relationships which may be considered as potential competing interests: